

# **Path-following Methods for a Class of Constrained Minimization Problems in Function Space**

**M. Hintermüller, K. Kunisch**

**RICAM-Report 2004-17**

# PATH-FOLLOWING METHODS FOR A CLASS OF CONSTRAINED MINIMIZATION PROBLEMS IN FUNCTION SPACE<sup>◊</sup>

M. HINTERMÜLLER\* AND K. KUNISCH<sup>†</sup>

ABSTRACT. Path-following methods for primal-dual active set strategies requiring a regularization parameter are introduced. Existence of a path and its differentiability properties are analyzed. Monotonicity and convexity of the primal-dual path value function are investigated. Both feasible and infeasible approximations are considered. Numerical path following strategies are developed and their efficiency is demonstrated by means of examples.

## 1. INTRODUCTION

Primal-dual active set strategies or, in some cases equivalently, semi-smooth Newton methods, were proven to be efficient methods for solving constrained variational problems in function space [1, 6, 7, 8, 9, 10]. In certain cases regularization parameters are required resulting in a family of approximating problems with more favorable properties than the original one, [9, 10]. In previous work convergence, and in some cases rate of convergence, with respect to the regularization parameter was proved. In the numerical work the adaptation of these parameters was heuristic, however. The focus of the present investigation is on an efficient control of the regularization parameter in the primal-dual active set strategy for a class of constrained variational problems. To explain the involved issues we proceed mostly formally in this section and consider the problem

$$(1) \quad \begin{cases} \min \mathcal{J}(v) & \text{over } v \in X \\ \text{s.t. } Gv \leq \psi, \end{cases}$$

---

*Date:* July 12, 2004.

\*Department of Computational and Applied Mathematics, Rice University, Houston, Texas.

<sup>†</sup>Institut für Mathematik, Karl-Franzens-Universität Graz, A-8010 Graz, Austria.

<sup>◊</sup>Research partially supported by the Fonds zur Förderung der wissenschaftlichen Forschung under SFB 03 „Optimierung und Kontrolle“.

where  $\mathcal{J}$  is a quadratic functional on a Hilbert space  $X$ , and  $G: X \rightarrow Y$ , with  $Y$  a Hilbert lattice induced by an ordering  $\leq$ , and  $\psi \in Y$ . We note that (1) subsumes problems of very different nature. For example, for  $\mathcal{J}(v) = \frac{1}{2} \int_{\Omega} |\nabla v|^2 dx - \int_{\Omega} f v$ , with  $\Omega$  a bounded domain in  $\mathbb{R}^n$ ,  $X = H_0^1(\Omega)$ , and  $G = I$  we obtain the classical obstacle problem. For the control constrained optimal control problem

$$\begin{cases} \min \frac{1}{2} |y - z|_{L^2}^2 + \frac{\alpha}{2} |u|_{L^2}^2 \\ \text{s.t. } -\Delta y = u \text{ in } \Omega, u = 0 \text{ on } \partial\Omega, \\ u \leq \psi, \end{cases}$$

with  $z \in L^2(\Omega)$ ,  $\alpha > 0$ , one can use  $y = (-\Delta)^{-1}u$ , where  $\Delta$  denotes the Laplacian with homogenous Dirichlet boundary conditions, and arrives at

$$\begin{cases} \min \frac{1}{2} |(-\Delta)^{-1}u - z|^2 + \frac{\alpha}{2} |u|^2 \\ \text{s.t. } u \leq \psi, \end{cases}$$

which is clearly of the form (1). For state constrained control problems with  $y \leq \psi$  one has

$$\begin{cases} \min \frac{1}{2} |(-\Delta)^{-1}u - z|^2 + \frac{\alpha}{2} |u|^2 \\ \text{s.t. } (-\Delta)^{-1}y \leq \psi, \end{cases}$$

which is also of the form (1). From the point of view of duality theory these three problems are very different. While it is straightforward to argue the existence of a Lagrange multiplier in  $L^2(\Omega)$  for the control constrained optimal control problem, it is already more involved and requires additional assumptions to guarantee its existence in  $L^2(\Omega)$  for obstacle problems, and for state constraint problems the Lagrange multiplier is only a measure. Formally we arrive in either of these cases at the optimality system of the form

$$(2) \quad \begin{cases} \mathcal{J}'(v) + \lambda = 0, \\ \lambda = \max(0, \lambda + c(G(v) - \psi)) \end{cases}$$

for any fixed  $c > 0$ . The second equation in (2) is equivalent to  $\lambda \geq 0$ ,  $G(v) \leq \psi$  and  $\lambda(G(v) - \psi) = 0$ .

The primal-dual active set strategy determines the active set at iteration level  $k$  by means of

$$\mathcal{A}_{k+1} = \{x \in \Omega: \lambda_k(x) + c(G(v_k)(x) - \psi(x)) > 0\},$$

assigns the inactive set  $\mathcal{I}_{k+1} = \Omega \setminus \mathcal{A}_{k+1}$ , and updates  $(v, \lambda)$  by means of

$$(3) \quad \begin{cases} \mathcal{J}'(v_{k+1}) + \lambda_{k+1} = 0, \\ \lambda_{k+1} = 0 \text{ on } \mathcal{I}_{k+1}, (G(v_{k+1}) - \psi)(x) = 0 \text{ for } x \in \mathcal{A}_{k+1}. \end{cases}$$

These auxiliary problems require special attention. For obstacle problems the constraint  $y_{k+1} = \psi$  on  $\mathcal{A}_{k+1}$  induces that the associated Lagrange multiplier  $\lambda_{k+1}$  is in general less regular than the Lagrange multiplier associated to  $y \leq \psi$  for the original problem. For problems with combined control and state constraints it may happen that (3) has no solution while the original problem does. For these reasons in earlier work the second equation in (2) was regularized resulting in the family of equations

$$(4) \quad \begin{cases} \mathcal{J}'(v) + \lambda = 0, \\ \lambda = \max(0, \bar{\lambda} + \gamma(G(v) - \psi)), \end{cases}$$

where  $\bar{\lambda}$  is fixed, possibly  $\bar{\lambda} = 0$ , and  $\gamma \in \mathbb{R}^+$ . It was shown that under appropriate conditions the solutions  $(v_\gamma, \lambda_\gamma)$  to (4) exist and converge to the solution of (2) as  $\gamma \rightarrow \infty^+$ .

In previous numerical implementations the increase of  $\gamma$  to infinity was heuristic. In this paper a framework for a properly controlled increase of  $\gamma$ -values will be developed. At the same time we aim at solving the auxiliary problems (3) only inexactly. Our work is inspired by concepts from path-following methods in finite dimensional spaces [3, 4, 12, 14, 15]. We first guarantee the existence of a sufficiently smooth path  $\gamma \rightarrow (y_\gamma, \lambda_\gamma)$ , with  $\gamma \in (0, \infty)$  in appropriately chosen function spaces. Once the path is available it can be used as the basis for updating-strategies of the path parameter. Given a current value  $\gamma_k$ , with associated primal and dual states  $(y_{\gamma_k}, \lambda_{\gamma_k})$ , the  $\gamma$ -update should be sufficiently large to make good progress towards satisfying the complementarity conditions. On the other hand, since we are not solving the problems along the path exactly, we have to use safeguards against steps which would lead us too far off the path. Of course, these goals are impeded by the fact that the path is not available numerically. To overcome this difficulty we use qualitative properties of the value function, like monotonicity and convexity, which can be verified analytically. These suggest the introduction of model functions which will be shown to approximate very well the value functional along the path. We use these model functions for our updating strategies of  $\gamma$ . In the case of exact path following we can even prove convergence of the resulting strategy. In the present paper the program just described

is carried out for a class of problems, corresponding to contact problems. State- constrained optimal control problems require a different approach that will be considered independently. As we shall see, the (infinite dimensional) parameter  $\bar{\lambda}$  can be used to guarantee that the iterates of the primal variable are feasible. As we shall see the numerical behavior of infeasible approximations is superior to the feasible ones from the point of view of iteration numbers.

Interior point methods also require an additional parameter, which, however enters into (2) differently. For the problem under consideration here, the interior-point relaxation replaces the second equation in (2) by

$$(5) \quad \lambda(x) (\psi - G(y))(x) = \frac{1}{\gamma} \text{ for } x \in \Omega.$$

Path following interior point methods typically start feasible, with iterates which are required to stay feasible during the iterations while satisfying, or satisfying approximately, the first equation in (2) and (5). Path-following interior point methods have not received much attention for infinite dimensional problems yet. In fact, we are only aware of [13], where such methods are analyzed for optimal control problems related to ordinary differential equations. For the problem classes that we outlined at the beginning of this section, the primal-dual active set strategy proved to be an excellent competitor to interior point methods, as was demonstrated, for example, in [1] comparing these two methods.

This paper is organized as follows. Section 2 contains the precise problem formulation and the necessary background on the primal-dual active set strategy. The existence and regularity of the primal-dual path is discussed in Section 3. Properties of the primal-dual path value functional are analyzed in Section 4. Section 5 contains the derivation of the proposed model functions for the primal-dual path value functional. Exact as well as inexact path-following algorithms are proposed in Section 6 and their numerical behavior is discussed there as well.

## 2. PROBLEM STATEMENT, REGULARIZATION AND ITS MOTIVATION

We consider

$$(P) \quad \begin{cases} \min \frac{1}{2} a(y, y) - (f, y) & \text{over } y \in H_0^1(\Omega) \\ \text{s.t. } y \leq \psi \end{cases}$$

where  $f \in L^2(\Omega)$ ,  $\psi \in H^1(\Omega)$ , with  $\psi|_{\partial\Omega} \geq 0$ , where  $\Omega$  is a bounded domain in  $\mathbb{R}^n$  with Lipschitz continuous boundary  $\partial\Omega$ . Throughout

$(\cdot, \cdot)$  denotes the standard  $L_2(\Omega)$ -inner product, and we assume that  $a(\cdot, \cdot)$  is a bilinear form on  $H_0^1(\Omega) \times H_0^1(\Omega)$  satisfying

$$(6) \quad a(v, v) \geq \nu |v|_{H_0^1}^2 \quad \text{and} \quad a(w, z) \leq \mu |w|_{H^1} |z|_{H^1}$$

for some  $\nu > 0$ ,  $\mu > 0$  independent of  $v \in H_0^1(\Omega)$  and  $w, z \in H^1(\Omega)$ . Moreover let  $A: H_0^1(\Omega) \rightarrow H^{-1}(\Omega)$  be defined by

$$a(v, w) = \langle Av, w \rangle_{H^{-1}, H_0^1} \quad \text{for all } v, w \in H_0^1(\Omega).$$

It is well-known that (P) admits a unique solution  $y^* \in H_0^1(\Omega)$  with associated Lagrange multiplier  $\lambda^* = -Ay^* + f$ , satisfying the optimality system

$$(7) \quad \begin{cases} a(y^*, v) + \langle \lambda^*, v \rangle_{H^{-1}, H_0^1} = (f, v), \\ \langle \lambda^*, y^* - \psi \rangle_{H^{-1}, H_0^1} = 0, y^* \leq \psi, \langle \lambda^*, v \rangle \leq 0 \text{ for all } v \leq 0. \end{cases}$$

This also holds with  $f \in H^{-1}(\Omega)$ . Under well-known additional requirements on  $a, \psi$  and  $\Omega$ , as for example

$$(8) \quad \begin{cases} a(v, w) = \int_{\Omega} (\sum a_{ij} v_{x_i} w_{x_j} + d v w), \quad \text{with } a_{ij} \in C^1(\bar{\Omega}), d \in L^\infty(\Omega), \\ \psi \in H^2(\Omega), \partial\Omega \text{ is } C^{1,1} \text{ or } \Omega \text{ is a polyhedron,} \end{cases}$$

we have  $(y^*, \lambda^*) \in H^2(\Omega) \times L^2(\Omega)$  and the optimality system can be expressed as

$$(9) \quad \begin{cases} Ay^* + \lambda^* = f \text{ in } L^2(\Omega), \\ \lambda^* = (\lambda^* + c(y^* - \psi))^+, \quad \text{for each } c > 0, \end{cases}$$

where  $(v)^+ = \max(0, v)$ .

Our aim is the development of Newton-type methods for solving (7) or (9) which is complicated by the system of inequalities in (7) and the non-differentiable max-operator in (9). In the recent past significant progress was made in the investigation of semi-smooth Newton methods and primal-dual active set methods to cope with non-differentiable functionals in infinite-dimensional spaces; see for instance [7, 11]. A direct application of these techniques to (9) results in the following algorithm.

### Algorithm A

- (i) Choose  $c > 0$ ,  $(y_0, \lambda_0)$ ; set  $k = 0$ .
- (ii) Set  $\mathcal{A}_{k+1} = \{x \in \Omega: \lambda_k(x) + c(y_k(x) - \psi(x)) > 0\}$ .
- (iii) Compute  $y_{k+1} = \arg \min \{\frac{1}{2} a(y, y) - (f, y): y = \psi \text{ on } \mathcal{A}_{k+1}\}$
- (iv) Let  $\lambda_{k+1}$  be the Lagrange multiplier associated to the constraint in (iii) with  $\lambda_{k+1} = 0$  on  $\Omega \setminus \mathcal{A}_{k+1}$ .

(v) Set  $k := k + 1$  and go to (ii).

The optimality system for the variational problem in (iii) is given by

$$(10) \quad \begin{cases} a(y_{k+1}, v) + \langle \lambda_{k+1}, v \rangle_{H^{-1}, H_0^1} = (f, v) \text{ for all } v \in H_0^1(\Omega), \\ y_{k+1} = \psi \text{ on } \mathcal{A}_{k+1}, \quad \lambda_{k+1} = 0 \text{ on } \mathcal{I}_{k+1} = \Omega \setminus \mathcal{A}_{k+1}. \end{cases}$$

The Lagrange multiplier associated to the constraint  $y = \psi$  on  $\mathcal{A}_{k+1}$  is in general only a distribution in  $H^{-1}(\Omega)$  and is not in  $L^2(\Omega)$ . In fact  $\lambda_{k+1}$  is related to the jumps in the normal derivatives of  $y$  across the interface between  $\mathcal{A}_{k+1}$  and  $\mathcal{I}_{k+1}$ , [10]. This complicates the convergence analysis for Algorithm A since the calculus of Newton differentiability [7] does not apply. We note that these difficulties are not present if (7) or (9) are discretized. However, they are crucial for the treatment of infinite dimensional problems and as such they are generic. Analogous difficulties arise for state constrained optimization problems, for inverse problems with BV-regularization, and for elasticity problems with contact and friction, to mention a few. This suggests the introduction of regularized problems, which in our case are chosen as

$$(P_\gamma) \quad \min \frac{1}{2} a(y, y) - \int_\Omega f y + \frac{1}{2\gamma} \int_\Omega |(\bar{\lambda} + \gamma(y - \psi))^+|^2 \text{ over } y \in H_0^1(\Omega)$$

where  $\gamma > 0$  and  $\bar{\lambda} \in L^2(\Omega)$ ,  $\bar{\lambda} \geq 0$  are fixed. For later use we denote the objective functional of  $(P_\gamma)$  by  $J(y; \gamma)$ . The choice of  $\bar{\lambda}$  will be used to influence the feasibility of the solution  $y_\gamma$  of  $(P_\gamma)$ . The first order optimality condition associated with  $(P_\gamma)$  is given by

$$(OC_\gamma) \quad \begin{cases} a(y_\gamma, v) + (\lambda_\gamma, v) = (f, v) \text{ for all } v \in H_0^1(\Omega), \\ \lambda_\gamma = (\bar{\lambda} + \gamma(y_\gamma - \psi))^+, \end{cases}$$

where  $(y_\gamma, \lambda_\gamma) \in H_0^1(\Omega) \times L^2(\Omega)$ . With (8) holding, we have  $y_\gamma \in H^2(\Omega)$ . The primal-dual active set strategy, or equivalently the semi-smooth Newton method, for  $(P_\gamma)$  is given next. For its statement and for later use we introduce  $\chi_{\mathcal{A}^{k+1}}$ , the characteristic function of the set  $\mathcal{A}^{k+1} \subseteq \Omega$ .

### Algorithm B

- (i) Choose  $\bar{\lambda} > 0$ ,  $(y_0, \lambda_0)$ ; set  $k = 0$ .
- (ii) Set  $\mathcal{A}_{k+1} = \{x \in \Omega: \bar{\lambda}(x) + \gamma(y_k(x) - \psi(x)) > 0\}$ ,  $\mathcal{I}_{k+1} = \Omega \setminus \mathcal{A}_{k+1}$ .
- (iii) Solve for  $y_{k+1} \in H_0^1(\Omega)$ :
 
$$a(y_{k+1}, v) + (\bar{\lambda} + \gamma(y_{k+1} - \psi), \chi_{\mathcal{A}_{k+1}} v) = (f, v), \text{ for all } v \in H_0^1(\Omega).$$

(iv) Set

$$\lambda_{k+1} = \begin{cases} 0 & \text{on } \mathcal{I}_{k+1}, \\ \bar{\lambda} + \gamma(y_{k+1} - \psi) & \text{on } \mathcal{A}_{k+1}. \end{cases}$$

Algorithm B was analyzed in [10] where global as well as locally superlinear convergence for every fixed  $\gamma > 0$  were established. The choice and adaptation (increase) of  $\gamma$  was heuristic in earlier work. The focus of the present investigation is the automatic adaptive choice of  $\gamma$ . We shall utilize the following two results which we recall from [10].

**Proposition 2.1.** *The solutions  $(y_\gamma, \lambda_\gamma)$  to  $(P_\gamma)$  converge to  $(y^*, \lambda^*)$  in the sense that  $y_\gamma \rightarrow y^*$  strongly in  $H_0^1(\Omega)$  and  $\lambda_\gamma \rightharpoonup \lambda^*$  weakly in  $H^{-1}(\Omega)$  as  $\gamma \rightarrow \infty$ .*

We say that  $a$  satisfies the weak maximum principle, if for any  $v \in H_0^1(\Omega)$

$$(11) \quad a(v, v^+) \leq 0 \text{ implies } v^+ = 0.$$

**Proposition 2.2.** *Assume that (11) holds and let  $0 < \gamma_1 \leq \gamma_2 < \infty$ .*

*a) In the infeasible case, i.e., for  $\bar{\lambda} = 0$ , we have  $y^* \leq y_{\gamma_2} \leq y_{\gamma_1}$ .*

*b) In the feasible case, i.e., if*

$$(12) \quad \bar{\lambda} \geq 0 \text{ and } \langle \bar{\lambda} - f + A\psi, v \rangle_{H^{-1}, H_0^1} \geq 0 \text{ for all } v \in H_0^1(\Omega),$$

*with  $v \geq 0$ , then  $y_{\gamma_1} \leq y_{\gamma_2} \leq y^* \leq \psi$ .*

### 3. THE PRIMAL-DUAL PATH

In this section we introduce the primal-dual path and discuss its smoothness properties.

**Definition 3.1.** *The family of solutions  $\mathcal{C} = \{(y_\gamma, \lambda_\gamma) : \gamma \in (0, \infty)\}$  to  $(OC_\gamma)$ , considered as subset of  $H_0^1(\Omega) \times H^{-1}(\Omega)$ , is called the primal-dual path associated to  $(P)$ .*

For  $r \geq 0$  we further set  $\mathcal{C}_r = \{(y_\gamma, \lambda_\gamma) : \gamma \in [r, \infty)\}$  and with some abuse of terminology we also refer to  $\mathcal{C}_r$  as path. In the following lemma we denote by  $\hat{y}$  the solution to the unconstrained problem

$$(\hat{P}) \quad \min J(y) = \frac{1}{2} a(y, y) - (f, y) \text{ over } y \in H_0^1(\Omega).$$

Subsequently, in connection with convergence of a sequence in function space we use the subscript 'weak' together with the space to indicate convergence in the weak sense.



**Lemma 3.1.** *For each  $r > 0$  the path  $\mathcal{C}_r$  is bounded in  $H_0^1(\Omega) \times H^{-1}(\Omega)$ , with  $\lim_{\gamma \rightarrow \infty} (y_\gamma, \lambda_\gamma) = (y^*, \lambda^*)$  in  $H_0^1(\Omega) \times H^{-1}(\Omega)_{weak}$ . For  $\bar{\lambda} = 0$  the path  $\mathcal{C}_0$  is bounded in  $H_0^1(\Omega) \times H^{-1}(\Omega)$ , with  $\lim_{\gamma \rightarrow 0^+} (y_\gamma, \lambda_\gamma) = (\hat{y}, 0)$  in  $H_0^1(\Omega) \times L^2(\Omega)$ .*

*Proof.* From (OC $_\gamma$ ) we have for every  $\gamma > 0$

$$(13) \quad a(y_\gamma, y_\gamma - y^*) + (\lambda_\gamma, y_\gamma - y^*) = (f, y_\gamma - y^*).$$

Since  $\lambda_\gamma = \max(0, \bar{\lambda} + \gamma(y_\gamma - \psi)) \geq 0$  and  $\psi - y^* \geq 0$  we have

$$\begin{aligned} (\lambda_\gamma, y_\gamma - y^*) &= (\lambda_\gamma, \frac{\bar{\lambda}}{\gamma} + y_\gamma - \psi + \psi - y^* - \frac{\bar{\lambda}}{\gamma}) \\ &\geq \frac{1}{\gamma} (\lambda_\gamma, \bar{\lambda} + \gamma(y_\gamma - \psi)) - \frac{1}{\gamma} (\lambda_\gamma, \bar{\lambda}) \\ &\geq \frac{1}{\gamma} [|\lambda_\gamma|_{L^2}^2 - (\lambda_\gamma, \bar{\lambda})]. \end{aligned}$$

Combined with (13) this implies that

$$(14) \quad a(y_\gamma, y_\gamma) + \frac{1}{\gamma} |\lambda_\gamma|_{L^2}^2 \leq a(y_\gamma, y^*) + (f, y_\gamma - y^*) + \frac{1}{\gamma} (\bar{\lambda}, \lambda_\gamma).$$

This estimate, (6) and (OC $_\gamma$ ) imply that  $\mathcal{C}_r$  is bounded in  $H_0^1(\Omega) \times H^{-1}(\Omega)$  for every  $r > 0$ . From Proposition 2.1 we have that  $\lim_{\gamma \rightarrow \infty} (y_\gamma, \lambda_\gamma) = (y^*, \lambda^*)$  in  $H_0^1(\Omega) \times H^{-1}(\Omega)_{weak}$ . If  $\bar{\lambda} = 0$ , then from (14), (6) and (OC $_\gamma$ ) the path  $\mathcal{C}_0$  is bounded in  $H_0^1(\Omega) \times H^{-1}(\Omega)$  and  $\lambda_\gamma \rightarrow 0$  in  $L^2(\Omega)$  for  $\gamma \rightarrow 0^+$ . From (OC $_\gamma$ ) and the optimality condition for ( $\hat{P}$ ) we have

$$a(y_\gamma - \hat{y}, y_\gamma - \hat{y}) + (\lambda_\gamma, y_\gamma - \hat{y}) = 0,$$

and hence  $\lim_{\gamma \rightarrow 0^+} y_\gamma = \hat{y}$  in  $H_0^1(\Omega)$ .  $\square$

**Proposition 3.1.** *The path  $\mathcal{C}_r$  is globally Lipschitz in  $H_0^1(\Omega) \times H^{-1}(\Omega)$ , for every  $r > 0$ . If  $\bar{\lambda} = 0$ , then  $\mathcal{C}_0$  is globally Lipschitz continuous.*

*Proof.* Let  $\gamma, \bar{\gamma} \in [r, \infty)$  be arbitrary. Then

$$A(y_\gamma - y_{\bar{\gamma}}) + (\bar{\lambda} + \gamma(y_\gamma - \psi))^+ - (\bar{\lambda} + \bar{\gamma}(y_{\bar{\gamma}} - \psi))^+ = 0.$$

Taking the inner-product with  $y_\gamma - \psi$  and using the Lipschitz continuity (with constant  $L = 1$ ) of  $x \rightarrow \max(0, x)$  we find

$$\begin{aligned} a(y_\gamma - y_{\bar{\gamma}}, y_\gamma - y_{\bar{\gamma}}) &\leq |((\bar{\lambda} + \gamma(y_\gamma - \psi))^+ - (\bar{\lambda} + \bar{\gamma}(y_{\bar{\gamma}} - \psi))^+, y_\gamma - y_{\bar{\gamma}})| \\ &\leq |\gamma - \bar{\gamma}| |y_\gamma - \psi|_{L^2} |y_\gamma - y_{\bar{\gamma}}|_{L^2}. \end{aligned}$$

By Lemma 3.1 the set  $\{y_\gamma\}_{\gamma \geq r}$  is bounded in  $H_0^1(\Omega)$ . Hence there exists  $K_1 > 0$  such that

$$\nu |y_\gamma - y_{\bar{\gamma}}|_{H_0^1}^2 \leq K_1 |\gamma - \bar{\gamma}| \cdot |y_\gamma - y_{\bar{\gamma}}|_{L^2}$$

and by Poincaré's inequality there exists  $K_2 > 0$  such that

$$|y_\gamma - y_{\bar{\gamma}}|_{H_0^1} \leq K_2 |\gamma - \bar{\gamma}| \quad \text{for all } \gamma \geq r, \bar{\gamma} \geq r.$$

Let us recall here that  $|y|_{H_0^1} = |\nabla y|_{L^2}$ . Lipschitz continuity of  $\gamma \rightarrow \lambda_\gamma$  from  $[r, \infty)$  to  $H^{-1}(\Omega)$  follows from the first equation in (OC $_\gamma$ ). For  $\bar{\lambda} = 0$  the set  $\{y_\gamma\}_{\gamma \geq 0}$  is bounded in  $H_0^1(\Omega)$ . The remainder of the proof remains identical.  $\square$

**Lemma 3.2.** *For every subset  $I \subset [r, \infty)$ ,  $r > 0$ , the mapping  $\gamma \rightarrow \lambda_\gamma$  is globally Lipschitz from  $I$  to  $L^2(\Omega)$ .*

*Proof.* For  $0 < \gamma_1 \leq \gamma_2$  we have by (OC $_\gamma$ )

$$\begin{aligned} |\lambda_{\gamma_1} - \lambda_{\gamma_2}|_{L^2} &= |(\bar{\lambda} + \gamma_1(y_{\gamma_1} - \psi))^+ - (\bar{\lambda} + \gamma_2(y_{\gamma_2} - \psi))^+| \\ &\leq (K_3 \gamma_1 + K_1 + |\psi|_{L^2}) |\gamma_1 - \gamma_2| \end{aligned}$$

for some constant  $K_3 > 0$ .  $\square$

We shall use the following notation:

$$S_\gamma = \{x \in \Omega : \bar{\lambda}(x) + \gamma(y_\gamma - \psi)(x) > 0\}.$$

Further we set

$$(15) \quad g(\gamma) = \bar{\lambda} + \gamma(y_\gamma - \psi).$$

Since  $\gamma \rightarrow y_\gamma \in H_0^1(\Omega)$  is Lipschitz continuous by Proposition 3.1, there exists a weak accumulation point  $\dot{y} (= \dot{y}_\gamma)$  of  $\frac{1}{\bar{\gamma} - \gamma}(y_{\bar{\gamma}} - y_\gamma)$  as  $\bar{\gamma} \rightarrow \gamma^+ > 0$ , which is also a strong accumulation point in  $L^2(\Omega)$ . Further  $\frac{1}{\bar{\gamma} - \gamma}(g(\bar{\gamma}) - g(\gamma))$  has  $\dot{g}(\gamma) := y_\gamma - \psi + \gamma \dot{y}_\gamma$  as strong accumulation point in  $L^2(\Omega)$  as  $\bar{\gamma} \rightarrow \gamma$ .

**Proposition 3.2.** *Let  $\gamma > 0$  and denote by  $\dot{y}_\gamma^+$  any weak accumulation point of  $\frac{1}{\bar{\gamma} - \gamma}(y_{\bar{\gamma}} - y_\gamma)$  in  $H_0^1(\Omega)$  as  $\bar{\gamma} \rightarrow \gamma^+$ . Set*

$$S_\gamma^+ = S_\gamma \cup \{x : \bar{\lambda}(x) + \gamma(y_\gamma(x) - \psi(x)) = 0 \wedge \dot{g}(\gamma)(x) \geq 0\}.$$

Then  $\dot{y}_\gamma^+$  satisfies

$$(16) \quad a(\dot{y}_\gamma^+, v) + ((y_\gamma - \psi + \gamma \dot{y}_\gamma^+) \chi_{S_\gamma^+}, v) = 0 \quad \text{for all } v \in H_0^1(\Omega).$$

*Proof.* By (OC $_\gamma$ ) we have for every  $v \in H_0^1(\Omega)$

$$(17) \quad a(y_{\bar{\gamma}} - y_\gamma, v) + ((\bar{\lambda} + \bar{\gamma}(y_{\bar{\gamma}} - \psi))^+ - (\bar{\lambda} + \gamma(y_\gamma - \psi))^+, v) = 0$$

We multiply (17) by  $(\bar{\gamma} - \gamma)^{-1}$  and discuss separately the two terms in (17). Clearly, we have

$$\lim_{\bar{\gamma} \rightarrow \gamma^+} (\bar{\gamma} - \gamma)^{-1} a(y_{\bar{\gamma}} - y_\gamma, v) = a(\dot{y}_\gamma^+, v).$$

Here and below the limit is taken on the sequence of  $\bar{\gamma}$ -values, which provides the accumulation point. Next by Lebesgue's bounded convergence theorem (and considering separately the cases  $g(\gamma)(x) < 0$ ,  $g(\gamma)(x) > 0$  and  $g(\gamma)(x) = 0$ ) we have

$$(18) \quad \begin{aligned} & (\bar{\gamma} - \gamma)^{-1}((g(\bar{\gamma})(x))^+ - (g(\gamma)(x))^+, v) \\ & \rightarrow ((y_\gamma - \psi + \gamma \dot{y}_\gamma^+) \chi_{S_\gamma^+}, v) \text{ as } \bar{\gamma} \rightarrow \gamma^+. \end{aligned}$$

□

As a consequence of the proof we obtain

**Corollary 3.1.** *Let  $\gamma > 0$  and denote by  $\dot{y}_\gamma^-$  any weak accumulation point of  $\frac{1}{\bar{\gamma} - \gamma}(y_{\bar{\gamma}} - y_\gamma)$  in  $H_0^1(\Omega)$  as  $\bar{\gamma} \rightarrow \gamma^-$ . Set  $S_\gamma^- = S_\gamma \cup \{x: \bar{\lambda}(x) + \gamma(y_\gamma(x) - \psi(x)) = 0 \wedge \dot{g}(\gamma)(x) \leq 0\}$ . Then  $\dot{y}_\gamma^-$  satisfies*

$$(19) \quad a(\dot{y}_\gamma^-, v) + ((y_\gamma - \psi + \gamma \dot{y}_\gamma^-) \chi_{S_\gamma^-}, v) = 0 \text{ for all } v \in H_0^1(\Omega).$$

Another corollary of Proposition 3.2 treats the case  $\bar{\lambda} = 0$ .

**Corollary 3.2.** *Let  $\bar{\lambda} = 0$  and assume that (11) holds. Then the right- and left derivatives  $\dot{y}_\gamma^+$  and  $\dot{y}_\gamma^-$  of  $\gamma \rightarrow y_\gamma$ ,  $\gamma \in (0, \infty)$  exist and are given by*

$$(20) \quad a(\dot{y}_\gamma^+, v) + ((y_\gamma - \psi + \gamma \dot{y}_\gamma^+) \chi_{y_\gamma > \psi}, v) = 0 \text{ for all } v \in H_0^1(\Omega)$$

$$(21) \quad a(\dot{y}_\gamma^-, v) + ((y_\gamma - \psi + \gamma \dot{y}_\gamma^-) \chi_{y_\gamma \geq \psi}, v) = 0 \text{ for all } v \in H_0^1(\Omega).$$

*Proof.* By Proposition 2.2 we have that

$$S_\gamma^+ = \{x \in \Omega: y_\gamma(x) > \psi(x)\} \cup \{x \in \Omega: y_\gamma(x) = \psi(x) \wedge \dot{y}_\gamma(x) = 0\}.$$

This implies that every accumulation point  $\dot{y}_\gamma^+$  satisfies (20). Since the solution to (20) is unique, the directional derivative from the right exists.

Similarly by Proposition 2.2 we have  $S_\gamma^- = \{x \in \Omega: y_\gamma(x) \geq \psi(x)\}$ , and (21) follows. □

Henceforth we set

$$S_\gamma^\circ = \{x \in \Omega: \bar{\lambda}(x) + \gamma(y_\gamma - \psi)(x) = 0\}.$$

**Corollary 3.3.** *If  $\text{meas}(S_\gamma^\circ) = 0$  then  $\gamma \rightarrow y_\gamma \in H_0^1(\Omega)$  is differentiable at  $\gamma$  and  $\dot{y}_\gamma$  satisfies*

$$(22) \quad a(\dot{y}_\gamma, v) + ((y_\gamma - \psi + \gamma \dot{y}_\gamma) \chi_{S_\gamma}, v) = 0 \text{ for all } v \in H_0^1(\Omega).$$

*Proof.* Let  $z$  denote the difference of two accumulation points of  $(\bar{\gamma} - \gamma)^{-1}(y_{\bar{\gamma}} - y_{\gamma})$  as  $\bar{\gamma} \rightarrow \gamma$ . As a consequence of (16) and (19)

$$a(z, v) + \gamma(z\chi_{S_{\gamma}}, v) = 0 \text{ for all } v \in H_0^1(\Omega).$$

This implies that  $z = 0$  by (6). Consequently, accumulation points are unique and by (16), (19) they satisfy (22).  $\square$

#### 4. THE PRIMAL-DUAL PATH VALUE FUNCTIONAL

In this section we investigate the value function associated with  $(P_{\gamma})$  and study its monotonicity as well as smoothness properties.

**Definition 4.1.** *The functional*

$$\gamma \rightarrow V(\gamma) = J(y_{\gamma}; \gamma)$$

*defined on  $(0, \infty)$  is called the primal-dual-path value functional.*

Let us start by studying first order differentiability properties of  $V$ .

**Proposition 4.1.** *The value function  $V$  is differentiable with*

$$\dot{V}(\gamma) = -\frac{1}{2\gamma^2} \int_{\Omega} |(\bar{\lambda} + \gamma(y_{\gamma} - \psi))^+|^2 + \frac{1}{\gamma} \int_{\Omega} (\bar{\lambda} + \gamma(y_{\gamma} - \psi))^+(y_{\gamma} - \psi).$$

**Corollary 4.1.** *For  $\bar{\lambda} = 0$  we have  $\dot{V}(\gamma) = \frac{1}{2} \int_{\Omega} |(y_{\gamma} - \psi)^+|^2 \geq 0$ , and  $\dot{V}(\gamma) > 0$  unless  $y_{\gamma}$  is feasible. For  $\bar{\lambda}$  satisfying (12) and with (11) holding we have  $y_{\gamma} \leq \psi$  and hence  $\dot{V}(\gamma) \leq 0$ , for  $\gamma \in (0, \infty)$ .*

*In either of the two cases  $\dot{V}(\gamma) = 0$  implies that  $y_{\gamma}$  solves  $(\hat{P})$ .*

*Proof.* We only show that  $\dot{V}(\gamma) = 0$  implies that  $y_{\gamma}$  solves  $(\hat{P})$ . The rest of the assertion follows immediately from Proposition 4.1.

If  $\bar{\lambda} = 0$ , then  $\dot{V}(\gamma) = 0$  yields  $y_{\gamma} \leq \psi$ . Thus,  $\lambda_{\gamma} = 0$  and, hence,  $y_{\gamma}$  solves  $(\hat{P})$ .

If (11) and (12) are satisfied, then  $y_{\gamma} \leq \psi$  and  $\dot{V}(\gamma) = 0$  implies  $\gamma(y_{\gamma} - \psi) \leq \bar{\lambda} + \gamma(y_{\gamma} - \psi) \leq 0$ . As a consequence  $\lambda_{\gamma} = 0$ , and  $y_{\gamma}$  solves  $(\hat{P})$ .  $\square$

*Proof (of Proposition 4.1).* For  $\bar{\gamma}, \gamma \in (0, \infty)$  we find

$$(23) \quad \begin{aligned} & \frac{1}{2} a(y_{\bar{\gamma}} + y_{\gamma}, y_{\bar{\gamma}} - y_{\gamma}) - (f, y_{\bar{\gamma}} - y_{\gamma}) + \\ & \frac{1}{2} ((\bar{\lambda} + \bar{\gamma}(y_{\bar{\gamma}} - \psi))^+ + (\bar{\lambda} + \gamma(y_{\gamma} - \psi))^+, y_{\bar{\gamma}} - y_{\gamma}) = 0, \end{aligned}$$

and consequently

$$\begin{aligned}
V(\bar{\gamma}) - V(\gamma) &= \frac{1}{2}a(y_{\bar{\gamma}}, y_{\bar{\gamma}}) - \frac{1}{2}a(y_{\gamma}, y_{\gamma}) - (f, y_{\bar{\gamma}} - y_{\gamma}) \\
&\quad + \frac{1}{2\bar{\gamma}} \int_{\Omega} |(\bar{\lambda} + \bar{\gamma}(y_{\bar{\gamma}} - \psi))^+|^2 - \frac{1}{2\gamma} \int_{\Omega} |(\bar{\lambda} + \gamma(y_{\gamma} - \psi))^+|^2 \\
&= \frac{1}{2\bar{\gamma}} \int_{\Omega} |(\bar{\lambda} + \bar{\gamma}(y_{\bar{\gamma}} - \psi))^+|^2 + \frac{1}{2\gamma} \int_{\Omega} -|(\bar{\lambda} + \gamma(y_{\gamma} - \psi))^+|^2 \\
&\quad + \frac{1}{2} \int_{\Omega} -((\bar{\lambda} + \bar{\gamma}(y_{\bar{\gamma}} - \psi))^+ + (\bar{\lambda} + \gamma(y_{\gamma} - \psi))^+)(y_{\bar{\gamma}} - y_{\gamma}) \\
&= \int_{P_{\bar{\gamma}} \cap P_{\gamma}} z + \int_{P_{\bar{\gamma}} \cap N_{\gamma}} z + \int_{P_{\gamma} \cap N_{\bar{\gamma}}} z = \mathcal{I}_1 + \mathcal{I}_2 + \mathcal{I}_3,
\end{aligned}$$

where  $z$  stands for the sum of the kernels on the left of the above equalities,

$$P_{\gamma} = \{x: \bar{\lambda} + \gamma(y_{\gamma} - \psi) > 0\}, N_{\gamma} = \{x: \bar{\lambda} + \gamma(y_{\gamma} - \psi) < 0\},$$

and  $P_{\bar{\gamma}}, N_{\bar{\gamma}}$  are defined analogously. For  $\mathcal{I}_2$  we have

$$\begin{aligned}
|\mathcal{I}_2| &\leq \frac{1}{2} \int_{P_{\bar{\gamma}} \cap N_{\gamma}} \frac{1}{\bar{\gamma}} (\bar{\lambda} + \bar{\gamma}(y_{\bar{\gamma}} - \psi))^2 + |\bar{\lambda} + \bar{\gamma}(y_{\bar{\gamma}} - \psi)| |y_{\bar{\gamma}} - y_{\gamma}| \\
&\leq \frac{1}{2} \int_{\Omega} \frac{1}{\bar{\gamma}} (\bar{\gamma}(y_{\bar{\gamma}} - \psi) - \gamma(y_{\gamma} - \psi))^2 + |y_{\bar{\gamma}} - y_{\gamma}| (|\bar{\gamma}y_{\bar{\gamma}} - \gamma y_{\gamma}| + |\bar{\gamma} - \gamma| |\psi|)
\end{aligned}$$

and hence by Proposition 3.1

$$(24) \quad \lim_{\bar{\gamma} \rightarrow \gamma} \frac{1}{\bar{\gamma} - \gamma} |\mathcal{I}_2| = 0.$$

Analogously one verifies that

$$(25) \quad \lim_{\bar{\gamma} \rightarrow \gamma} \frac{1}{\bar{\gamma} - \gamma} |\mathcal{I}_3| = 0.$$

On  $P_{\bar{\gamma}} \cap P_{\gamma}$  we have

$$\begin{aligned}
z &= \frac{1}{2\bar{\gamma}} (\bar{\lambda} + \bar{\gamma}(y_{\bar{\gamma}} - \psi))^2 \\
&\quad - \frac{1}{2\gamma} (\bar{\lambda} + \gamma(y_{\gamma} - \psi))^2 - \frac{1}{2} (2\bar{\lambda} + \bar{\gamma}(y_{\bar{\gamma}} - \psi) + \gamma(y_{\gamma} - \psi))(y_{\bar{\gamma}} - y_{\gamma}) \\
&= \frac{\bar{\gamma} - \gamma}{2\bar{\gamma}\gamma} (\bar{\lambda} + \bar{\gamma}(y_{\bar{\gamma}} - \psi))^2 \\
&\quad + \frac{1}{2\bar{\gamma}} [2\bar{\lambda}(\bar{\gamma}(y_{\bar{\gamma}} - \psi) - \gamma(y_{\gamma} - \psi)) + \bar{\gamma}^2(y_{\bar{\gamma}} - \psi)^2 - \gamma^2(y_{\gamma} - \psi)^2] \\
&\quad - \frac{1}{2} (2\bar{\lambda} + \bar{\gamma}(y_{\bar{\gamma}} - \psi) + \gamma(y_{\gamma} - \psi))(y_{\bar{\gamma}} - y_{\gamma}) \\
&= \frac{\bar{\gamma} - \gamma}{2\bar{\gamma}\gamma} (\bar{\lambda} + \bar{\gamma}(y_{\bar{\gamma}} - \psi))^2 + \frac{\bar{\lambda}}{\gamma} [\bar{\gamma}(y_{\bar{\gamma}} - \psi) - \gamma(y_{\gamma} - \psi)] \\
&\quad + \frac{1}{2} \left[ \frac{\bar{\gamma}^2}{\gamma} (y_{\bar{\gamma}} - \psi)^2 - \bar{\gamma}(y_{\bar{\gamma}} - \psi)^2 + (\bar{\gamma} - \gamma)(y_{\bar{\gamma}} - \psi)(y_{\gamma} - \psi) \right]
\end{aligned}$$

and thus on  $P_{\bar{\gamma}} \cap P_{\gamma}$

$$\begin{aligned} (\bar{\gamma} - \gamma)^{-1}z &= \frac{-1}{2\bar{\gamma}\gamma}(\bar{\lambda} + \bar{\gamma}(y_{\gamma} - \psi))^2 + \frac{\bar{\lambda}}{\gamma}(y_{\bar{\gamma}} - \psi) \\ &\quad + \frac{1}{2} \left[ \frac{\bar{\gamma}}{\gamma}(y_{\bar{\gamma}} - \psi)^2 + (y_{\bar{\gamma}} - \psi)(y_{\gamma} - \psi) \right]. \end{aligned}$$

By Lebesgue's bounded convergence theorem

$$\begin{aligned} \lim_{\bar{\gamma} \rightarrow \gamma} \frac{1}{\bar{\gamma} - \gamma} \mathcal{I}_1 &= \lim_{\bar{\gamma} \rightarrow \gamma} \frac{1}{\bar{\gamma} - \gamma} \int_{\Omega} z \chi_{P_{\bar{\gamma}} \cap P_{\gamma}} \\ &= -\frac{1}{2\gamma^2} \int_{\Omega} ((\bar{\lambda} + \gamma(y_{\gamma} - \psi))^+)^2 + \frac{1}{\gamma} \int_{\Omega} (\bar{\lambda} + \gamma(y_{\gamma} - \psi))^+(y_{\gamma} - \psi). \end{aligned}$$

Together with (24) and (25) this implies the claim.  $\square$

**Remark 4.1.** Note that  $\dot{V}$  is characterized without recourse to  $y_{\gamma}$ .

The boundedness of  $\{\gamma^2 \dot{V}(\gamma)\}_{\gamma \geq 0}$  is established next.

**Proposition 4.2.** If  $\bar{\lambda} = 0$  and  $a(v^+, v^-) = 0$  for all  $v \in H_0^1(\Omega)$ , then  $\{\gamma^2 \dot{V}(\gamma)\}_{\gamma \geq 0}$  is bounded. If (11) and (12) hold, then again  $\{\gamma^2 \dot{V}(\gamma)\}_{\gamma \geq 0}$  is bounded.

*Proof.* In the case  $\bar{\lambda} = 0$  we have

$$a(y_{\gamma} - \psi, v) + \gamma((y_{\gamma} - \psi)^+, v) = (f, v) - a(\psi, v) \text{ for all } v \in H_0^1(\Omega).$$

Since  $(y_{\gamma} - \psi) \in H_0^1(\Omega)$  and  $a((y_{\gamma} - \psi)^+, (y_{\gamma} - \psi)^-) = 0$  we have, using (6) with  $v = (y_{\gamma} - \psi)^+$

$$\nu |(y_{\gamma} - \psi)^+|_{H_0^1(\Omega)}^2 + \gamma |(y_{\gamma} - \psi)^+|_{L^2}^2 \leq |f|_{L^2} |(y_{\gamma} - \psi)^+|_{H_0^1} + \mu |\psi|_{H^1} |y_{\gamma} - \psi|_{H^1}.$$

This implies the existence of a constant  $K$ , depending on  $|\psi|_{H^1}$  and  $|f|_{L^2}$ , but independent of  $\gamma \geq 0$ , such that  $\gamma |(y_{\gamma} - \psi)^+|_{L^2} \leq K$ . Since  $\dot{V}(\gamma) = \frac{1}{2} \int_{\Omega} |(y_{\gamma} - \psi)^+|^2$  the claim follows.

Turning to the feasible case with (11) and (12) holding, we have that  $y_{\gamma} \leq \psi$  for every  $\gamma > 0$ , and hence  $(\bar{\lambda} + \gamma(y_{\gamma} - \psi))(x) > 0$  if and only if  $\bar{\lambda}(x) > \gamma(\psi - y_{\gamma})(x)$ . Consequently,

$$\begin{aligned} |\dot{V}(\gamma)| &\leq \frac{1}{2\gamma^2} \int_{\Omega} |(\bar{\lambda} + \gamma(y_{\gamma} - \psi))^+|^2 + \frac{1}{\gamma} \int_{\Omega} (\bar{\lambda} + \gamma(y_{\gamma} - \psi))^+(\psi - y_{\gamma}) \\ &\leq \frac{3}{2\gamma^2} |\bar{\lambda}|_{L^2}^2, \end{aligned}$$

which again implies the claim.  $\square$

Before we investigate  $\ddot{V}$ , we state a result which connects  $\gamma \dot{V}(\gamma)$ ,  $|y^* - y_{\gamma}|_{H_0^1}$ , and  $V^* - V(\gamma)$ , where  $V^* = \lim_{\gamma \rightarrow \infty} V(\gamma)$ .

**Proposition 4.3.** *The following estimate holds true:*

$$|y^* - y_\gamma|_{H_0^1}^2 \leq \frac{2}{\nu} \left( V^* - V(\gamma) - \gamma \dot{V}(\gamma) \right).$$

*Proof.* We have  $V^* - V(\gamma) = J(y^*; \gamma) - J(y_\gamma; \gamma)$  and

$$\begin{aligned} J(y^*; \gamma) - J(y_\gamma; \gamma) &\geq \frac{\nu}{2} |y^* - y_\gamma|_{H_0^1}^2 + a(y_\gamma, y^* - y_\gamma) - (f, y^* - y_\gamma) \\ &\quad + \frac{1}{2\gamma} |(\bar{\lambda} + \gamma(y^* - \psi))^+|_{L^2}^2 - \frac{1}{2\gamma} |(\bar{\lambda} + \gamma(y_\gamma - \psi))^+|_{L^2}^2 \end{aligned}$$

where we used (6). From (OC $_\gamma$ ) we have

$$a(y_\gamma, y^* - y_\gamma) - (f, y^* - y_\gamma) = -((\bar{\lambda} + \gamma(y_\gamma - \psi))^+, y^* - y_\gamma),$$

and hence

$$\begin{aligned} J(y^*; \gamma) - J(y_\gamma; \gamma) &\geq \frac{\nu}{2} |y^* - y_\gamma|_{H_0^1}^2 \\ &\quad - \frac{1}{\gamma} ((\bar{\lambda} + \gamma(y_\gamma - \psi))^+, -(\bar{\lambda} + \gamma(y_\gamma - \psi)) + \bar{\lambda} + \gamma(y^* - \psi)) \\ &\quad + \frac{1}{2\gamma} |(\bar{\lambda} + \gamma(y^* - \psi))^+|_{L^2}^2 - \frac{1}{2\gamma} |(\bar{\lambda} + \gamma(y_\gamma - \psi))^+|_{L^2}^2 \\ &\geq \frac{\nu}{2} |y^* - y_\gamma|_{H_0^1}^2 - \frac{1}{2\gamma} |(\bar{\lambda} + \gamma(y_\gamma - \psi))^+|_{L^2}^2 \\ &\quad - \frac{1}{\gamma} ((\bar{\lambda} + \gamma(y_\gamma - \psi))^+, \bar{\lambda}) + \frac{1}{\gamma} |(\bar{\lambda} + \gamma(y_\gamma - \psi))^+|_{L^2}^2 \\ &= \frac{\nu}{2} |y^* - y_\gamma|_{H_0^1}^2 - \frac{1}{2\gamma} |(\bar{\lambda} + \gamma(y_\gamma - \psi))^+|_{L^2}^2 \\ &\quad + ((\bar{\lambda} + \gamma(y_\gamma - \psi))^+, y_\gamma - \psi) \\ &= \frac{\nu}{2} |y^* - y_\gamma|_{H_0^1}^2 + \gamma \dot{V}(\gamma). \end{aligned}$$

This proves the assertion.  $\square$

Below we shall assume that  $y_\gamma - \psi \in C(\bar{\Omega})$ . Recall that for  $n \leq 3$  and with (6) and (8) holding, we have  $y_\gamma \in H^2(\Omega) \subset C(\bar{\Omega})$ .

**Proposition 4.4.** *Let  $\dot{\gamma}$  denote any accumulation point of  $(\bar{\gamma} - \gamma)^1 (y_{\bar{\gamma}} - y_\gamma)$  as  $\bar{\gamma} \rightarrow \gamma$ .*

- (a) *If  $\bar{\lambda} = 0$ ,  $y_\gamma - \psi \in C(\bar{\Omega})$  and (8) is satisfied, then  $\gamma \rightarrow V(\gamma)$  is twice differentiable at  $\gamma$  with*

$$(26) \quad \ddot{V}(\gamma) = \int_{\Omega} (y_\gamma - \psi)^+ \dot{\gamma}_\gamma.$$

(b) For arbitrary  $\bar{\lambda}$ , if  $\text{meas}(S_\gamma^\circ) = 0$ , then  $\gamma \rightarrow V(\gamma)$  is twice differentiable at  $\gamma$  with

$$(27) \quad \begin{aligned} \ddot{V}(\gamma) = & \frac{1}{\gamma^3} \int_{\Omega} |(\bar{\lambda} + \gamma(y_\gamma - \psi))^+|^2 - \\ & \frac{2}{\gamma^2} \int_{\Omega} (\bar{\lambda} + \gamma(y_\gamma - \psi))^+ (y_\gamma - \psi) + \\ & \frac{1}{\gamma} \int_{\Omega} (y_\gamma - \psi)(y_\gamma - \psi + \gamma \dot{y}_\gamma) \chi_{S_\gamma}. \end{aligned}$$

*Proof.* (a) On the subsequence  $\gamma_n$  realizing the accumulation point, we have that  $\lim_{n \rightarrow \infty} (\gamma_n - \gamma)^{-1} (\dot{V}(\gamma_n) - \dot{V}(\gamma))$  equals the right hand side of (26). The claim will be established by verifying that the accumulation points  $\dot{y}_\gamma$  restricted to  $S_\gamma = \{x : y_\gamma(x) - \psi(x) > 0\}$  are unique. Let  $z$  denote the difference of two accumulation points. By (16) and (19) we have

$$a(z, v) + \gamma(z, v) = 0 \text{ for all } v \in H_0^1(\Omega) \text{ with } v = 0 \text{ on } \Omega \setminus S_\gamma.$$

Using (8) and the fact that  $S_\gamma$  is an open set relative to  $\Omega$  due to continuity of  $y_\gamma - \psi$ , we find that  $z = 0$  in  $S_\gamma$ , as desired.

(b) Let  $\dot{y}_\gamma$  denote any accumulation point of  $(\bar{\gamma} - \gamma)^{-1}(y_{\bar{\gamma}} - y_\gamma)$  as  $\bar{\gamma} \rightarrow \gamma^+$ , and recall the notation  $g(\gamma) = \bar{\lambda} + \gamma(y_\gamma - \psi)$  and  $S_\gamma^+$  from section 3. On the subsequence realizing the accumulation point we find

$$(28) \quad \begin{aligned} \lim_{\bar{\gamma} \rightarrow \gamma} \frac{1}{\bar{\gamma} - \gamma} (\dot{V}(\bar{\gamma}) - \dot{V}(\gamma)) = & \frac{1}{\gamma^3} \int_{\Omega} |(\bar{\lambda} + \gamma(y_\gamma - \psi))^+|^2 \\ & - \frac{2}{\gamma^2} \int_{\Omega} (\bar{\lambda} + \gamma(y_\gamma - \psi))^+ (y_\gamma - \psi) \\ & + \frac{1}{\gamma} \int_{\Omega} (y_\gamma - \psi)(y_\gamma - \psi + \gamma \dot{y}_\gamma) \chi_{S_\gamma^+}. \end{aligned}$$

By assumption,  $\text{meas}(S_\gamma^\circ) = 0$  and, hence, the right hand sides of (27) and (28) coincide. Since  $\dot{y}_\gamma$  is unique by Corollary 3.3 the claim is established.  $\square$

## 5. MODEL FUNCTIONS

In this section we derive low-parameter families of functions which approximate the value functional  $V$  and share some of its qualitative properties. We will make use of these models in the numerics section when devising path following algorithms.

**5.1. Infeasible case.** Throughout this subsection we assume

$$(29) \quad \bar{\lambda} = 0, y_\gamma - \psi \in C(\bar{\Omega}) \text{ for all } \gamma \in (0, \infty), \text{ and (8).}$$



Observe that (8), together with the general assumption (6), imply (11). In fact, for any  $v \in H_0^1(\Omega)$  we have  $a(v, v^+) \geq \gamma|v^+|^2$  and hence  $0 \geq a(v, v^+)$  implies  $v^+ = 0$ .

**Proposition 5.1.**  $\dot{V}(\gamma) \geq 0$  and  $\ddot{V}(\gamma) \leq 0$  for  $\gamma \in (0, \infty)$ .

*Proof.* Proposition 4.1 implies that  $\dot{V}(\gamma) \geq 0$ . Moreover  $y_{\gamma_2} \leq y_{\gamma_1}$  and hence  $\dot{y}_\gamma \leq 0$  a.e. on  $S_\gamma$ . Consequently  $\ddot{V}(\gamma) \leq 0$  by Proposition 4.4.  $\square$

A model function  $m$  for the value function  $V$  should reflect the sign properties of  $V$ . Moreover  $V(0)$  gives the value of  $(\hat{P})$  and hence we shall require that  $m(0) = V(0)$ . Finally from Lemma 3.1 we conclude that  $V$  is bounded on  $[0, \infty)$ . All these properties are satisfied by functions of the form

$$(30) \quad m(\gamma) = C_1 - \frac{C_2}{E + \gamma}$$

with  $C_1 \in \mathbb{R}$ ,  $C_2 \geq 0$ ,  $E > 0$  satisfying

$$(31) \quad m(0) = V(0) = C_1 - \frac{C_2}{E}.$$

Other choices for model functions are also conceivable, for example,  $\gamma \rightarrow C_1 - \frac{C_2}{(E+\gamma)^r}$  with  $r > 1$ . Note, however, that the asymptotic behavior of the model in (30) is such that  $\gamma^2 \dot{m}(\gamma)$  is bounded for  $\gamma \rightarrow \infty$ . This is consistent with the boundedness of  $\gamma^2 \dot{V}(\gamma)$  for  $\gamma \rightarrow \infty$  asserted in Proposition 4.1.

Another reason for choosing (30) is illustrated next. Choosing  $v = \max(0, y_\gamma - \psi)$  in (OC $_\gamma$ ) we find

$$(32) \quad a(\dot{y}_\gamma, \max(0, y_\gamma - \psi)) + |\max(0, y_\gamma - \psi)|_{L^2}^2 + \gamma \int_\Omega \max(0, y_\gamma - \psi) \dot{y}_\gamma = 0.$$

We

$$(33) \quad \text{replace } a(\cdot, \cdot) \text{ by } E(\cdot, \cdot) \text{ with } E \text{ a positive constant, and } V \text{ by } m.$$

By Proposition 4.1 and (26) the following ordinary differential equation is obtained for  $m$ :

$$(34) \quad (E + \gamma) \ddot{m}(\gamma) + 2 \dot{m}(\gamma) = 0.$$

The solutions to (34) are given by (30). To get an account for the quality of our model in (30) we refer to Figure 3 in Section 6.

5.2. **Feasible case.** Throughout this subsection we assume

$$(35) \quad (11), \bar{\lambda} \text{ satisfies (12) and } \text{meas}(S_\gamma^\circ) = 0 \text{ for all } \gamma \in (0, \infty).$$

**Proposition 5.2.**  $\dot{V}(\gamma) \leq 0$  and  $\ddot{V}(\gamma) \geq 0$  for  $\gamma \in (0, \infty)$ .

*Proof.* By Proposition 2.2 we have  $y_\gamma \leq \psi$  and hence  $\dot{V}(\gamma) \leq 0$  by Proposition 4.1. A short computation based on (27) shows that

$$(36) \quad \ddot{V}(\gamma) = \frac{1}{\gamma^3} \int_{\Omega} \chi \bar{\lambda}^2 + \int_{\Omega} \chi (y_\gamma - \psi) \dot{y}_\gamma \geq \frac{1}{\gamma} \int_{\Omega} \chi (y_\gamma - \psi)^2 + \int_{\Omega} \chi (y_\gamma - \psi) \dot{y}_\gamma,$$

where  $\chi$  is the characteristic function of the set  $S_\gamma = \{\bar{\lambda} + \gamma(y_\gamma - \psi) > 0\}$ . From (22) we have

$$\gamma |\dot{y}_\gamma|_{L^2(S_\gamma)} \leq |\psi - y_\gamma|_{L^2(S_\gamma)},$$

and hence  $\ddot{V}(\gamma) \geq 0$ .  $\square$

An immediate consequence is stated next.

**Lemma 5.1.** *If the solution to the unconstrained problem is not feasible, then  $\lim_{\gamma \rightarrow 0^+} V(\gamma) = \infty$ .*

*Proof.* Assume that  $\lim_{\gamma \rightarrow 0^+} V(\gamma)$  is finite. Then, using  $(P_\gamma)$ , there exists a sequence  $\gamma_n \rightarrow 0$  and  $\tilde{y} \in H_0^1(\Omega)$  such that  $y_{\gamma_n} \rightharpoonup \tilde{y}$  weakly in  $H_0^1(\Omega)$ , with  $y_{\gamma_n}$  the solution to  $(P_{\gamma_n})$ , and  $\lambda_{\gamma_n} = \max(0, \bar{\lambda} + \gamma_n(y_n - \psi)) \rightarrow 0$  in  $L^2(\Omega)$ . Consequently  $\tilde{y} \leq \psi$ . Taking the limit with respect to  $n$  in  $(OC_{\gamma_n})$  it follows that  $\tilde{y} \leq \psi$  is the solution to  $(\hat{P})$  which contradicts our assumption.  $\square$

From Lemmas 3.1 and 5.1, and Proposition 5.2 it follows that  $\gamma \rightarrow V(\gamma)$ ,  $\gamma \in (0, \infty)$ , is a monotonically strictly decreasing, convex function with  $\lim_{\gamma \rightarrow 0^+} V(\gamma) = \infty$ . All these properties are also satisfied by functions of the form

$$(37) \quad m(\gamma) = C_1 - \frac{C_2}{E + \gamma} + \frac{B}{\gamma},$$

provided that  $C_1 \in \mathbb{R}$ ,  $C_2 \geq 0$ ,  $E > 0$ ,  $B > 0$  and  $C_2 \leq B$ .

We now give the motivation for choosing the model function  $m$  for  $V$  as in (37). From (22) with  $v = (y_\gamma - \psi)\chi$

$$a(\dot{y}_\gamma, (y - \psi)\chi) + \gamma(\dot{y}_\gamma \chi, y_\gamma - \psi) + \gamma((y_\gamma - \psi)\chi, y_\gamma - \psi) = 0,$$

where  $\chi = \chi_{S_\gamma}$ . As in the infeasible case we replace  $a(\cdot, \cdot)$  by  $E(\cdot, \cdot)$ , with  $E$  a constant, and using (22) we arrive at

$$(E + \gamma)(\dot{y}_\gamma \chi, v) + ((y_\gamma - \psi)\chi, v) = 0.$$

The choice  $v = y_\gamma - \psi$  implies

$$(38) \quad (E + \gamma)(\dot{y}_\gamma \chi, y_\gamma - \psi) + ((y_\gamma - \psi)\chi, y_\gamma - \psi) = 0.$$

Note that  $\dot{V}(\gamma)$  can be expressed as

$$(39) \quad \dot{V}(\gamma) = -\frac{1}{2\gamma^2} \int_{\Omega} \bar{\lambda}^2 \chi + \frac{1}{2} \int_{\Omega} (y_\gamma - \psi)^2 \chi.$$

Using (36) and (39) in (38), and replacing  $V$  by  $m$ , due to the substitution for  $a(\cdot, \cdot)$ , we find

$$(E + \gamma)\dot{m} + 2\dot{m} - E\gamma^{-3} \int_{\Omega} \chi \bar{\lambda} = 0.$$

We further replace  $\int_{\Omega} \chi \bar{\lambda}$ , which is a bounded quantity depending on  $\gamma$ , by  $2B$ , and obtain, as the ordinary differential equation that we propose for the model function  $m$  in the feasible case,

$$(40) \quad (E + \gamma)\dot{m} + 2\dot{m} - 2\gamma^{-3}EB = 0.$$

The family of solutions is given by (37). In Figure 4 in Section 6 we study the approximation quality of  $m(\gamma)$ .

## 6. PATH-FOLLOWING ALGORITHMS

In this section we study the basic Algorithm B together with a variety of adjustment schemes for the path parameter  $\gamma$ . For this purpose recall that, depending on the shift parameter  $\bar{\lambda}$ , the elements  $y_\gamma$  along the primal-dual path are feasible or infeasible. As we have seen in the previous section, this implies different models for approximating the value function  $V$ . We will see, however, that for  $\gamma > 0$  in both cases similar strategies for updating  $\gamma$  may be used. When referring to the infeasible or feasible case, (29), respectively, (35) is assumed to hold.

The subsequent discussion is based on the following two-dimensional test problems.

**Test problem P1.** We consider (8) with  $a_{ij} = 1$ ,  $d = 0$  and  $\Omega = (0, 1)^2$ . We choose

$$f(x_1, x_2) = 500x_1 \sin(5x_1) \cos(x_2)$$

and  $\psi \equiv 10$  on  $\Omega \setminus K$ , and  $\psi \equiv 1$  on  $K$  with  $K = \{x \in \Omega : \frac{1}{5} \leq \|x - (\frac{1}{2}, \frac{1}{2})^\top\|_2 \leq \frac{2}{5}\}$ . The solution  $y^*$ , the obstacle  $\psi$ , and the active set  $\mathcal{A}^*$  at the solution are shown in Figure 1.

**Test problem P2.** Again we consider (8) with  $a_{ij}$ ,  $d$  and  $\Omega$  as before,

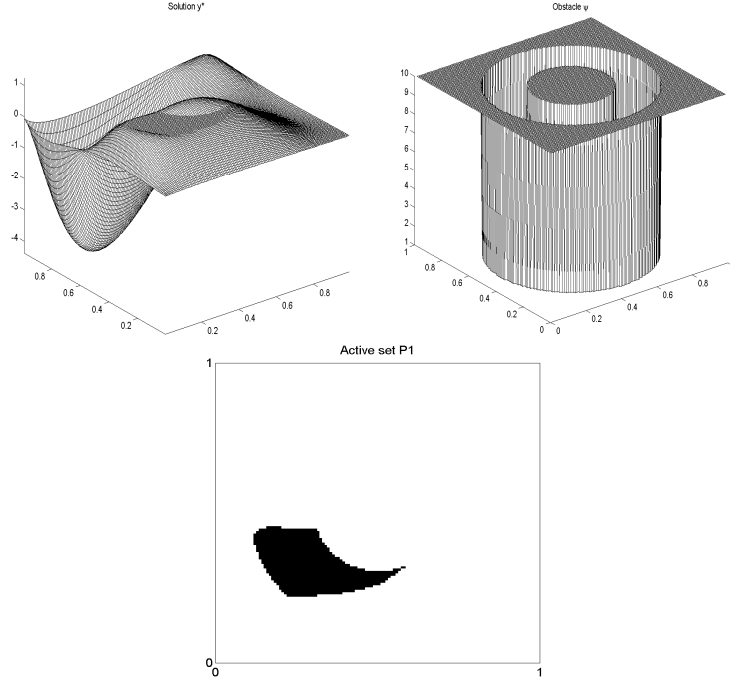


FIGURE 1. Optimal solution  $y^*$  (upper left plot), obstacle  $\psi$  (upper right plot), and the active set  $\mathcal{A}^*$  (lower plot) for test problem 1.

and define

$$(41) \quad y^\dagger := \begin{cases} x_1 & \text{on } T_1 := \{x \in \Omega : x_2 \leq x_1 \wedge x_2 \leq 1 - x_1\}, \\ 1 - x_2 & \text{on } T_2 := \{x \in \Omega : x_2 \leq x_1 \wedge x_2 \geq 1 - x_1\}, \\ 1 - x_1 & \text{on } T_3 := \{x \in \Omega : x_2 \geq x_1 \wedge x_2 \geq 1 - x_1\}, \\ x_2 & \text{on } T_4 := \{x \in \Omega : x_2 \geq x_1 \wedge x_2 \leq 1 - x_1\}. \end{cases}$$

The obstacle  $\psi$  is defined by  $\psi \equiv y^\dagger$  on  $S_1 := \{x \in \Omega : \|x - (\frac{1}{2}, \frac{1}{2})^\top\|_\infty \leq \frac{1}{4}\}$ ,  $\psi \equiv \frac{1}{4}$  on  $S_2 \setminus S_1$ , and

$$\psi := \begin{cases} 2x_1 & \text{on } T_1 \cap (\Omega \setminus S_2), \\ \frac{1}{4} - 2(x_2 - \frac{7}{8}) & \text{on } T_2 \cap (\Omega \setminus S_2), \\ \frac{1}{4} - 2(x_1 - \frac{7}{8}) & \text{on } T_3 \cap (\Omega \setminus S_2), \\ 2x_2 & \text{on } T_4 \cap (\Omega \setminus S_2), \end{cases}$$

with  $S_2 := \{x \in \Omega : \|x - (\frac{1}{2}, \frac{1}{2})^\top\|_\infty \leq \frac{3}{8}\}$ . The forcing term is given by

$$(f, \phi)_{L^2} = \int_{\Omega^+} \phi(s) ds + (\chi_{S_1}, \phi)_{L^2} + \int_{S_1 \cap \Omega^+} \phi(s) ds \text{ for all } \phi \in H_0^1(\Omega),$$

where  $\Omega^+ := \{x \in \Omega : x_2 = x_1\} \cup \{x \in \Omega : x_2 = -x_1\}$ . We recall that for  $\phi \in H_0^1(\Omega)$ ,  $\Omega \subset \mathbb{R}^2$ , the traces along smooth curves are well-defined. The solution  $y^*$  is given by  $y^* = y^\dagger$ . The active or coincidence set at the solution is  $\mathcal{A}^* = S_1$ . The Lagrange multiplier  $\lambda^* = f + \Delta y^*$  is in  $H^{-1}(\Omega)$  and enjoys no extra regularity. In Figure 2 we display the optimal solution  $y^*$  (upper left plot), the obstacle  $\psi$  (upper right plot), and the active set  $\mathcal{A}^*$  (lower plot).

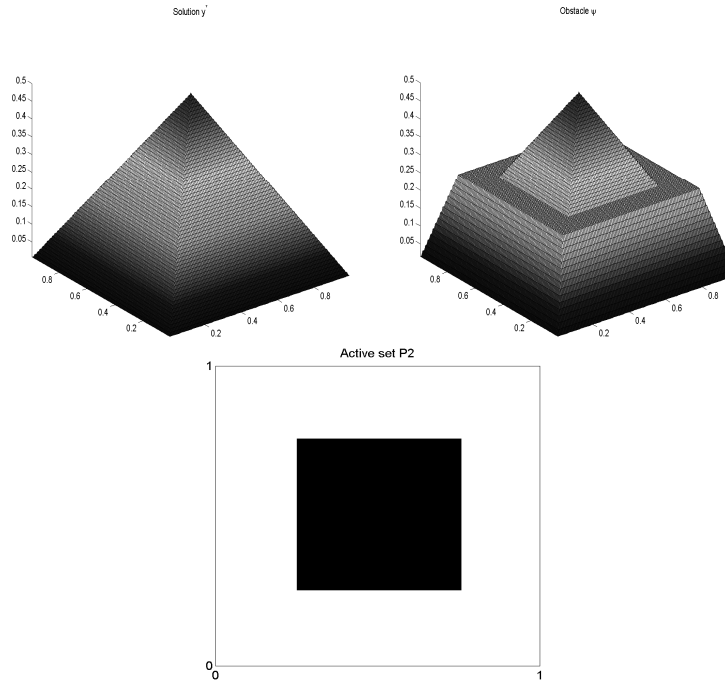


FIGURE 2. Optimal solution  $y^*$  (upper left plot), obstacle  $\psi$  (upper right plot), and the active set  $\mathcal{A}^*$  (lower plot) for test problem 2.

Unless specified otherwise, the subsequent algorithms are initialized by  $y_0 = (-\Delta)^{-1}f$ , where  $-\Delta$  denotes the Laplacian with homogeneous Dirichlet boundary conditions. The initial Lagrange multiplier is chosen as  $\lambda_0 = \gamma_0 \chi_{\{y_0 > \psi\}}(y_0 - \psi)$ .

The discretization of  $-\Delta$  is based on the classical five point finite difference stencil. By  $h$  we denote the mesh size which we occasionally drop for convenience. The forcing term  $f$  in  $P2$  is discretized by  $f = -\Delta y^\dagger + \chi_{S_1} e + \chi_{S_1} (-\Delta y^\dagger)$ , where  $e$  is the vector of all ones, and  $\chi_{S_1}$  represents a diagonal matrix with entry  $(\chi_{S_1})_{ii} = 1$  for grid points  $x_i \in S_1$  and  $(\chi_{S_1})_{ii} = 0$  otherwise. Above  $y^\dagger$  denotes the grid function corresponding to (41).

**6.1. A strategy based on model functions – exact path following.** As outlined in section 5 there are good reasons to trust our model functions (30) and (37) in the infeasible and feasible cases, respectively. Let us start by focusing on the infeasible case. The model is given by  $m(\gamma) = C_1 - C_2(E + \gamma)^{-1}$ . For determining the three parameters  $C_1, C_2$  and  $E$ , we use the information  $V(0), V(\gamma), \dot{V}(\gamma)$ , which, by Proposition 4.1, is available from one solve of the unconstrained problem ( $\hat{P}$ ) and one solve for ( $P_\gamma$ ). The conditions

$$(42) \quad m(0) = V(0), \quad m(\gamma) = V(\gamma), \quad \dot{m}(\gamma) = \dot{V}(\gamma)$$

yield

$$(43) \quad \begin{aligned} E &= \gamma^2 \dot{V}(\gamma) \left( V(\gamma) - V(0) - \gamma \dot{V}(\gamma) \right)^{-1}, \\ C_2 &= \gamma^{-1} E (E + \gamma) (V(\gamma) - V(0)), \\ C_1 &= V(0) + C_2 E^{-1}. \end{aligned}$$

We could have used an alternative reference value  $\gamma_r \in (0, \gamma)$  and computed  $m(\gamma_r) = V(\gamma_r)$  instead of  $m(0) = V(0)$ . In Figure 3 we compare  $V(\gamma)$  to  $m(\gamma)$  for different values of the coefficients  $(C_1, C_2, E)$ . These coefficients depend on different values for  $\gamma$  (in (42)) produced by Algorithm EPTS (see below) for problem  $P1$ . The solid line corresponds to  $V(\gamma)$ . The corresponding  $\gamma$ -values for (42) are depicted in the legend of Figure 3. The dotted and dashed line belong to rather small  $\gamma$ -values and the dashed-dotted and the circled lines to large  $\gamma$  in (42). As we can see, the dotted line is accurate in the range for relatively small  $\gamma$ , while the other lines are more accurate for large  $\gamma$ .

Now observe that  $m(\gamma) \leq C_1$  and  $m(\gamma) \rightarrow C_1$  for  $\gamma \rightarrow +\infty$ . Assume that the solution  $\hat{y}$  to ( $\hat{P}$ ) is not feasible for (P). Then by Corollary 4.1 we have  $\dot{V}(\gamma) > 0$  for all  $\gamma > 0$ . Consequently  $V(\gamma) < V(0)$  and  $V(\gamma) - V(0) - \gamma \dot{V}(\gamma) = -\int_0^\gamma \int_s^\gamma \ddot{V}(\sigma) d\sigma ds > 0$ , and, hence,  $E > 0$  and  $C_2 > 0$  for all  $\gamma \in (0, +\infty)$ .

We propose the following update strategy for  $\gamma$ : Let  $\{\tau_k\}$  satisfy  $\tau_k \in (0, 1)$  for all  $k \in \mathbb{N}$  and  $\tau_k \downarrow 0$  as  $k \rightarrow \infty$ , and assume that  $V(\gamma_k)$  is available. Then, given  $\gamma_k$  the updated value  $\gamma_{k+1}$  should ideally satisfy

$$(44) \quad |V^* - V(\gamma_{k+1})| \leq \tau_k |V^* - V(\gamma_k)|.$$

Since  $V^*$  and  $V(\gamma_{k+1})$  are unknown, we use  $C_{1,k}$  and our model  $m_k(\gamma) = C_{1,k} - C_{2,k}/(E_k + \gamma)$  at  $\gamma = \gamma_{k+1}$  instead. Thus, (44) is replaced by

$$(45) \quad |C_{1,k} - m_k(\gamma_{k+1})| \leq \tau_k |C_{1,k} - V(\gamma_k)| =: \beta_k.$$

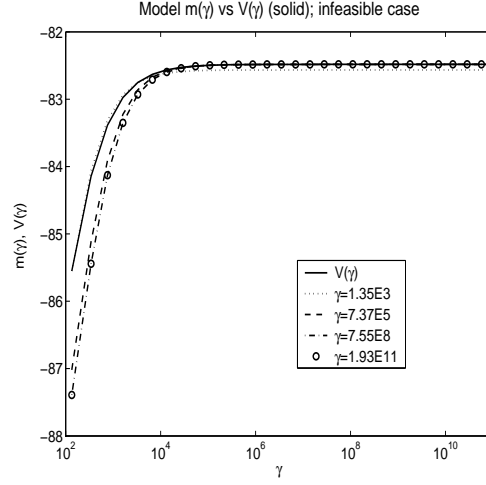


FIGURE 3. Model  $m(\gamma)$  vs.  $V(\gamma)$  (solid) in the infeasible case.

Solving the equation  $C_{1,k} - m_k(\gamma_{k+1}) = \beta_k$ , we obtain

$$(46) \quad \gamma_{k+1} = \frac{C_{2,k}}{\beta_k} - E_k.$$

In Theorem 6.1 we shall show that  $\gamma_{k+1} \geq \kappa \gamma_k$ , with  $\kappa > 1$ , independently of  $k \in \mathbb{N}$ .

In the feasible case, *i.e.*, when  $\bar{\lambda}$  satisfies (12), we use the model  $m(\gamma) = C_1 - C_2(E + \gamma)^{-1} + B\gamma^{-1}$  with  $C_2 \geq 0$  and  $E, B > 0$ ; see (37). Let  $\gamma_r > 0$ ,  $\gamma_r \neq \gamma$ , denote a reference  $\gamma$ -value, then we use the conditions

$$m(\gamma_r) = V(\gamma_r), \quad \dot{m}(\gamma_r) = \dot{V}(\gamma_r), \quad m(\gamma) = V(\gamma), \quad \dot{m}(\gamma) = \dot{V}(\gamma).$$

Solving the corresponding system of nonlinear equations, we get

$$E = \frac{\left( (\gamma_r - \gamma)(\dot{V}(\gamma_r)\gamma_r^2 + \dot{V}(\gamma)\gamma^2) + 2\gamma_r\gamma(V(\gamma) - V(\gamma_r)) \right)}{\left( (\dot{V}(\gamma)\gamma + \dot{V}(\gamma_r)\gamma_r)(\gamma - \gamma_r) + (\gamma_r + \gamma)(V(\gamma_r) - V(\gamma)) \right)}$$

and

$$B = \frac{\gamma_r^2 \gamma^2 \left( (V(\gamma) - V(\gamma_r))^2 - \dot{V}(\gamma)\dot{V}(\gamma_r)(\gamma - \gamma_r)^2 \right)}{\left( (\gamma - \gamma_r)^2 (\dot{V}(\gamma_r)\gamma_r^2 + \dot{V}(\gamma)\gamma^2) + 2(\gamma - \gamma_r)\gamma_r\gamma(V(\gamma_r) - V(\gamma)) \right)}$$

Then the parameters  $C_1$  and  $C_2$  are given by

$$C_2 = (E + \gamma)^2 \left( \frac{B}{\gamma^2} + \dot{V}(\gamma) \right),$$

$$C_1 = V(\gamma) + \frac{C_2}{E + \gamma} - \frac{B}{\gamma}.$$

In Figure 4 we plot  $|m(\gamma) - V(\gamma)|$  with  $m(\gamma)$  produced by the iterates of Algorithm EPTS for  $P1$  similar to the infeasible case. Again we can see that our model yields a close approximation of the value function  $V$ .

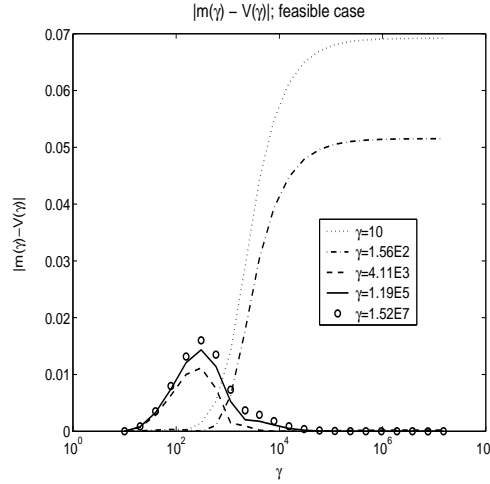


FIGURE 4. Model  $m(\gamma)$  vs.  $V(\gamma)$  in the feasible case.

If we require that (45) is satisfied in the feasible case, then we obtain the following update strategy for  $\gamma$ :

$$(47) \quad \gamma_{k+1} = -\frac{D_k}{2} + \sqrt{\frac{D_k^2}{4} + \frac{B_k E_k}{\beta_k}},$$

where  $D_k = E_k + (C_{2,k} - B_k)/\beta_k$ . In Theorem 6.1 we shall establish  $\gamma_{k+1} \geq \kappa \gamma_k$  for all  $k \in \mathbb{N}_0$  with  $\kappa > 1$  independent of  $k$ .

Next we describe an **exact path-following** version of Algorithm B which utilizes the update strategy (45) for updating  $\gamma$ .

**Algorithm EP.**

- (i) Select  $\gamma_r$ . Compute  $V(\gamma_r)$  and choose  $\gamma_0 > \max(1, \gamma_r)$ ; set  $k = 0$ .
- (ii) Apply Algorithm B to obtain  $y_{\gamma_k}$ .



- (iii) Compute  $V(\gamma_k)$ ,  $\dot{V}(\gamma_k)$  and  $\gamma_{k+1}$  according to (46) in the infeasible case or (47) in the feasible case.
- (iv) Set  $k = k + 1$ , and go to (ii).

Concerning the choice of  $\gamma_r$  note that in the infeasible case we have  $\gamma_r \geq 0$ , and in the feasible case  $\gamma_r > 0$ . Convergence of Algorithm EP is addressed next.

**Theorem 6.1.** *Assume that the solution to  $(\hat{P})$  is not feasible for (P). Then the iterates  $\gamma_k$  of Algorithm EP tend to  $\infty$  as  $k \rightarrow \infty$  and consequently  $\lim_{k \rightarrow \infty} (y_{\gamma_k}, \lambda_{\gamma_k}) = (y^*, \lambda^*)$ .*

*Proof.* Let us consider the infeasible case. then (45) is equivalent to

$$(48) \quad 0 < C_{1,k} - m_k(\gamma_{k+1}) < \tau_k(C_{1,k} - m(\gamma_k)).$$

Since  $\gamma \rightarrow m(\gamma)$  is strictly increasing and  $\tau_k \in (0, 1)$ , it follows that  $\gamma_{k+1} > \gamma_k$  for every  $k = 0, 1, \dots$ . If  $\lim_{k \rightarrow \infty} \gamma_k = \infty$ , then  $\lim_{k \rightarrow \infty} (y_{\gamma_k}, \lambda_{\gamma_k}) = (y^*, \lambda^*)$ . Otherwise there exists  $\bar{\gamma}$  such that  $\lim_{k \rightarrow \infty} \gamma_k = \bar{\gamma}$ . Since  $\gamma \rightarrow V(\gamma)$  and  $\gamma \rightarrow \dot{V}(\gamma)$  are continuous on  $(0, \infty)$ , it follows from (42) and (43) that  $\lim_{k \rightarrow \infty} E_k = E(\bar{\gamma})$ ,  $\lim_{k \rightarrow \infty} C_{1,k} = C_1(\bar{\gamma})$ , and  $\lim_{k \rightarrow \infty} C_{2,k} = C_2(\bar{\gamma})$ , where  $E(\bar{\gamma})$ ,  $C_1(\bar{\gamma})$ ,  $C_2(\bar{\gamma})$  are given by (43) with  $\gamma$  replaced by  $\bar{\gamma}$ . Taking the limit with respect to  $k$  in (48) we arrive at

$$\frac{C_2(\bar{\gamma})}{E(\bar{\gamma}) + \bar{\gamma}} = 0,$$

which is impossible, since  $C_2(\bar{\gamma}) > 0$  and  $E(\bar{\gamma}) > 0$  if the solution to  $(\hat{P})$  is not feasible for (P). Thus  $\lim_{k \rightarrow \infty} \gamma_k = \infty$ . The feasible case is treated analogously.  $\square$

Numerically we stop the algorithm as soon as  $\|(r_k^{1,h}, r_k^{2,h}, r_k^{3,h})^\top\|_2 \leq \sqrt{\epsilon_M}$ , where

$$\begin{aligned} r_k^{1,h} &= \|y_{\gamma_k}^h + (-\Delta^h)^{-1}(\lambda_{\gamma_k}^h - f^h)\|_{L_2^h} / \|f^h\|_{L_2^h}, \\ r_k^{2,h} &= \|\lambda_{\gamma_k}^h - \max(0, \lambda_{\gamma_k}^h + y_{\gamma_k}^h - \psi^h)\|_{L_2^h}, \\ r_k^{3,h} &= \|\max(0, y_{\gamma_k}^h - \psi^h)\|_{L_2^h}, \end{aligned}$$

$\epsilon_M$  denotes the machine accuracy and  $\|\cdot\|_{L_2^h}$  the discrete  $L^2$ -norm; see [5]. The inner iteration, *i.e.*, Algorithm B for  $\gamma = \gamma^k$  is terminated if successive active sets coincide or

$$\|-\Delta y_{\gamma_k}^{h,l} + \lambda_{\gamma_k}^{h,l} - f^h\|_{L_2^h} / \|f^h\|_{L_2^h} \leq \sqrt{\epsilon_M}.$$

Here the superscript  $l = l(k)$  denotes the iteration index of Algorithm B for fixed  $k$ .

The initialization of  $\gamma$  is as follows: In the infeasible case we set  $\gamma_r = 0$ , compute  $y_0, V(0)$  and  $\dot{V}(0)$ . Then we set

$$(49) \quad \gamma_0 = \max \left\{ 1, \zeta \frac{\hat{J}(y_b) - V(0)}{\dot{V}(0)} \right\},$$

where  $\zeta \in (0, 1]$  is some fixed constant,  $y_b(x) = \min(y_0(x), \psi(x))$ , and  $\hat{J}$  denotes the objective function of  $(\hat{P})$ . Note that  $y_0$  is the minimizer of the unconstrained problem  $(\hat{P})$ . For the examples below we used  $\zeta = 1$ . In the feasible case we choose a reference value  $\gamma_r$ , e.g.,  $\gamma_r = 1$ , and solve the path problem  $(P_\gamma)$ . Then we choose

$$(50) \quad \gamma_0 = \gamma_r + \frac{\hat{J}(\hat{y}) - V(\gamma_r)}{\dot{V}(\gamma_r)},$$

where  $\hat{y}$  denotes the minimizer of the discretized unconstrained problem  $(\hat{P})$ . If  $\hat{y}$  is not feasible for (P), then one has  $\hat{J}(\hat{y}) < V(\gamma_r)$  and hence  $\gamma_0 > \gamma_r$ .

When applied to P1 and P2 for  $h = 1/128$  and with  $\tau_k = 0.01^{k+1}$ , we obtain the results shown in Figure 5 and Table 1.

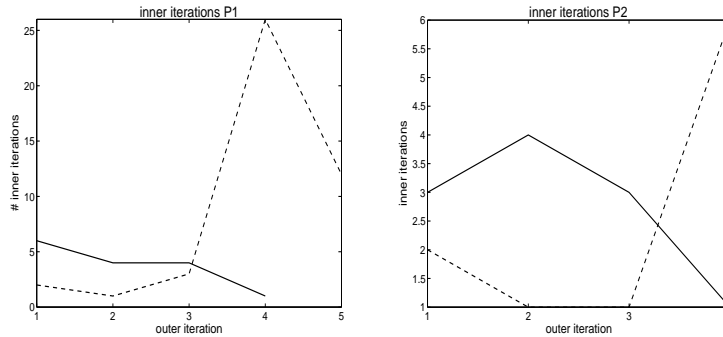


FIGURE 5. Number of inner iterations (vertical axis) per outer iteration for P1 (left plot) and P2 (right plot); solid line – infeasible case; dashed line – feasible case.

version	P1		P2	
	# outer it.	# inner it.	# outer it.	# inner it.
feasible	5	44	4	10
infeasible	4	15	4	11

TABLE 1. Comparison of iteration counts.

From our test runs we observe the following characteristics:

- For the feasible version the number of inner iterations increases until a saturation value is reached and then starts to decrease. For the infeasible version we typically observe that the first couple of iterations require several inner iterations. As the outer iterations proceed the number of inner iterations drops eventually to one. This behavior is also true for less aggressive  $\gamma$ -updates compared to the ones used here.
- The numerically observable convergence speed of  $y_{\gamma_k}$  towards  $y^*$  in  $H_0^1(\Omega)$  is typically superlinear. This can be seen from Figure 6 where the plots for the discrete versions of the quotients

$$q_k = \frac{|y_{\gamma_{k+1}} - y^*|_{H_0^1}}{|y_{\gamma_k} - y^*|_{H_0^1}}$$

are shown. Note the  $y$ -scale is a logarithmic one.

- In connection with the convergence speed it is of interest how the detection process of the correct active set works. For the rather aggressive  $\gamma$ -updates used in Algorithm EP the difference between two successive active sets is zero typically only in the last iteration. However, if a less aggressive strategy for updating  $\gamma$  is used, then it is to expect, that the difference of active sets might become zero already earlier along the iteration. In Figure 7, for the strategy  $\gamma_{k+1} = 2\gamma_k$ , we show the difference of successive active sets, *i.e.*, the vertical axis relates to the number of grid point which are in  $\mathcal{A}_{k+1}$  but not in  $\mathcal{A}_k$  and vice versa. We detect that for the infeasible case there exists an iteration index  $\bar{k}$  after which the difference is constantly zero. This behavior is a strong indication that the correct active set was detected. It suggests to fix this set  $\mathcal{A}_{\bar{k}}$ , and to set  $\bar{y}_{|\mathcal{A}_{\bar{k}}} = \psi_{|\mathcal{A}_{\bar{k}}}$ ,  $\bar{\mathcal{I}}_{\bar{k}} = \Omega \setminus \mathcal{A}_{\bar{k}}$  and  $\bar{\lambda}_{\bar{\mathcal{I}}_{\bar{k}}} = 0$ . Then one computes  $\bar{y}_{|\bar{\mathcal{I}}_{\bar{k}}}$  and  $\bar{\lambda}_{\bar{\mathcal{A}}_{\bar{k}}}$  such that  $a(\bar{y}, v) + \langle \bar{\lambda}, v \rangle_{H^{-1}, H_0^1} = (f, v)$  for all  $v \in H_0^1(\Omega)$  and checks whether  $(\bar{y}, \bar{\lambda})$  satisfies (7). If this is the case, then the solution is found; otherwise  $\gamma_{\bar{k}}$  is updated and the iteration continued. If we apply this technique for  $P1$  in the infeasible case, then the algorithm stops at iteration 15 (35 inner iterations) with the exact discrete solution as compared to 28 outer and 47 inner iterations without the additional stopping rule. There were four iterations where the additional system solve was necessary but without obtaining the numerical solution. Hence, w.r.t. system solves the amount of work drops from 47 solves to 39 (= 35 + 4). A similar observation is true for  $P2$ . In the feasible case, however, this strategy yields no reduction of iterations.

Here, typically the correct active set is determined in the last iteration (for large enough  $\gamma$ ).

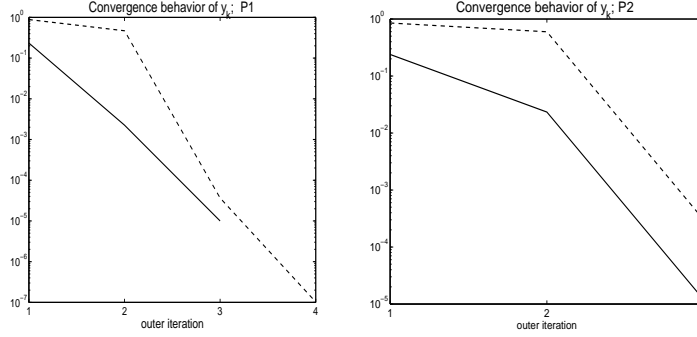


FIGURE 6. Discrete quotients  $q_k$  for  $P1$  and  $P2$ ; solid line – infeasible case; dashed line – feasible case.

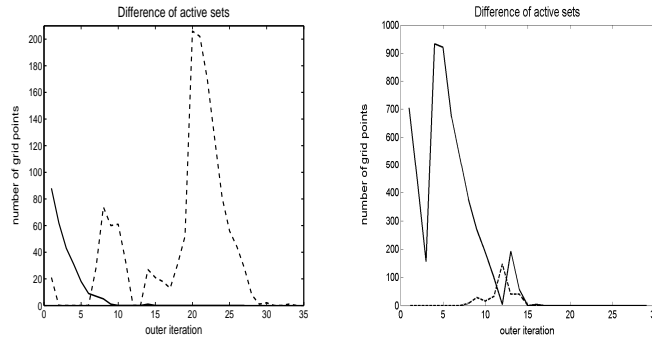


FIGURE 7. Difference in active sets for  $P1$  and  $P2$ ; solid line – infeasible case; dashed line – feasible case.

- The dependence of the iteration number on the mesh size of the discretization for  $P1$  are depicted in Table 2 (the ones for  $P2$  are similar). In parenthesis we show the number of inner iterations. The results clearly indicate that the outer iterations are mesh independent, while the number of inner iterations increases as the mesh size decreases.
- From the plots in Figure 8, where the  $y$ -axis again has a logarithmic scale, it can be seen that our strategy (45) produces a rapidly increasing sequence  $\{\gamma_k\}$ . The plots in Figure 8 depict the increase of  $\gamma_k$  as a function of the iteration number. The question arises, whether one could increase  $\gamma$  more rapidly. Numerical examples employing an ad-hoc strategy show that if  $\gamma$

	Mesh size $h$				
version	1/16	1/32	1/64	1/128	1/256
EP feasible	5(19)	5(23)	5(30)	5(44)	5(72)
EP infeasible	4(8)	4(11)	4(13)	4(15)	4(19)

TABLE 2. Comparison of iteration counts for different mesh sizes.

is increased too quickly, then the numerical error may prevent the residuals of the first order system to drop below  $\sqrt{\epsilon_M}$ . On the other hand, small increases in  $\gamma$  result in a slow convergence speed of Algorithm EP. Further, in our test runs and as can be seen from Figure 8 the feasible version of Algorithm EP was less aggressive in enlarging  $\gamma_k$ .

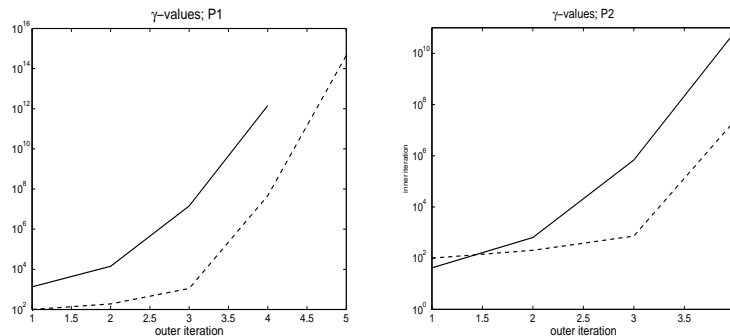


FIGURE 8.  $\gamma$ -updates; solid line – infeasible case; dashed line – feasible case.

**6.2. Inexact path following.** While exact path following is primarily of theoretical interest, the development of inexact path following techniques which keep the number of iterations as small as possible is of more practical importance. The strategy in the previous section relies on the fact that for every  $\gamma_k$  the corresponding point on the primal-dual path is computed. This, however, is not the case for inexact techniques and, as a consequence, a different update strategy for the path parameter  $\gamma$  is necessary. A common concept in inexact path-following methods is based on the definition of an appropriate neighborhood of the path; see, *e.g.*, [2] and the references therein for a non-interior neighborhood-based path-following method, or [4, 12, 14, 15] for path-following techniques related to interior point methods. It is typically required that the primal-dual iterates stay within the neighborhood of

the path, with the goal to reduce the computational burden while still maintaining convergence of the method.

We define

$$(51a) \quad r_\gamma^1(y, \lambda) = \| -\Delta y + \lambda - f \|_{H_0^1},$$

$$(51b) \quad r_\gamma^2(y, \lambda) = \| \lambda - \max(0, \lambda + \gamma(y - \psi)) \|_{L^2},$$

and the neighborhood:

$$(52) \quad \mathcal{N}(\gamma) := \{(y, \lambda) \in H_0^1(\Omega) \times L^2(\Omega) : \|(r_\gamma^1(y, \lambda), r_\gamma^2(y, \lambda))^\top\|_2 \leq \frac{\tau}{\gamma}\}$$

in the infeasible case and

$$(53) \quad \mathcal{N}(\gamma) := \{(y, \lambda) \in H_0^1(\Omega) \times L^2(\Omega) : \|(r_\gamma^1(y, \lambda), r_\gamma^2(y, \lambda))^\top\|_2 \leq \frac{\tau}{\gamma} \wedge \frac{\partial}{\partial \gamma} J(y; \gamma) \leq 0\}$$

in the feasible case. Above  $\tau > 0$  denotes some fixed parameter.

Next we specify our framework for an **inexact path following** algorithm.

### Algorithm IP.

- (i) Initialize  $\gamma_0$  according to (49) in the infeasible case or (50) in the feasible case; set  $k := 0$ .
- (ii) Apply Algorithm B to find  $(y_{k+1}, \lambda_{k+1}) \in \mathcal{N}(\gamma_k)$ .
- (iii) Update  $\gamma_k$  to obtain  $\gamma_{k+1}$ .
- (iv) Set  $k = k + 1$ , and go to (ii).

Note that if in step (ii) the path-problem  $(P_\gamma)$  is solved, then  $r_\gamma^1(y_\gamma, \lambda_\gamma) = r_\gamma^2(y_\gamma, \lambda_\gamma) = 0$ .

As it is the case with primal-dual path-following interior point methods, the update strategy for  $\gamma$  in step (iii) of Algorithm IP is a delicate issue. If the increase of  $\gamma$  from one iteration to the next is rather small, then we follow the path closely and the convergence speed is slow. If the  $\gamma$ -update is too aggressive, then step (ii) requires many iterations of Algorithm B to produce iterates in the neighborhood. We propose the following strategy which performed very well in our numerical tests.

We introduce the *primal infeasibility measure*  $\rho^F$ , and the *complementarity measure*  $\rho^C$  as follows

$$(54) \quad \rho_{k+1}^F := \int_{\Omega} (y_{k+1} - \psi)^+ dx,$$

$$(55) \quad \rho_{k+1}^C := \int_{\mathcal{I}_{k+1}} (y_{k+1} - \psi)^+ dx + \int_{\mathcal{A}_{k+1}} (y_{k+1} - \psi)^- dx,$$

where  $(\cdot)^- = -\min(0, \cdot)$  and  $(\cdot)^+ = \max(0, \cdot)$ . Note that at the optimal solution both measures vanish. Note that  $\rho^C$  is related to the duality measure well-known from primal-dual path following interior point methods. These measures are used in the following criterion for updating  $\gamma$ :

$$(56) \quad \gamma_{k+1} \geq \max \left( \gamma_k \max \left( \tau_1, \frac{\rho_{k+1}^F}{\rho_{k+1}^C} \right), \frac{1}{(\max(\rho_{k+1}^F, \rho_{k+1}^C))^q} \right)$$

with  $\tau_1 > 1$ , and  $q \geq 1$ . The first term in the outermost max-expression is used because of our observation that  $\rho_{k+1}^F \geq \rho_{k+1}^C$  in the infeasible case. If  $\rho^C$  is small compared to  $\rho^F$  we find that the iterates primarily lack feasibility as compared to complementarity. Therefore, a strong increase in  $\gamma$  which aims at reducing constraint infeasibility is favorable. If both measures are of almost the same size and rather small, then the second term in the outer max expression should yield a significant increase in  $\gamma$ . Typically  $q \in [\frac{3}{2}, 2]$  is chosen which induces growth rates for  $\gamma$ .

If there is still a significant change in the active sets from one iteration to the next and the update  $\gamma_{k+1}$  based on (56) would be too large compared to  $\gamma_k$ , then many inner iterations would be necessary to keep track of the path or very conservative  $\gamma$ -updates in the following iterations have to be chosen. We safeguard the  $\gamma$ -updates by utilizing our model function  $m(\gamma)$ , which was found to be a reliable tool. In fact, in updating  $\gamma$  large deviations from  $m(\gamma)$  are prohibited by comparing the value of the tangent to  $J(y; \gamma)$  at  $\gamma = \gamma_k$  with the actual model value. If necessary and as long as  $\gamma_{k+1}$  is much larger than  $\gamma_k$ , we reduce the actual  $\gamma$ -value until

$$(57) \quad |t_k(\gamma_{k+1}) - m_k(\gamma_{k+1})| \leq \tau_3 |J(y_{k+1}; \gamma_k) - J(y_k; \gamma_{k-1})|$$

with  $0 < \tau_3 < 1$ ,  $t_k(\gamma) = J(y_{k+1}; \gamma_k) + \frac{\partial J}{\partial \gamma}(y_{k+1}; \gamma_k)(\gamma - \gamma_k)$ , and  $m_k(\gamma)$  the model related to  $\gamma_k$ . Recall that  $m_k(\gamma_k) = J(y_{k+1}; \gamma_k)$ . The motivation of this strategy utilizes the good approximation qualities of our models. Indeed, for small  $\gamma$  the distance between  $t_k$  and  $m_k$  might be large, but so is  $|J(y_{k+1}; \gamma_k) - J(y_k; \gamma_{k-1})|$  since the change in the

function value is expected to be relatively large for small  $\gamma$ . For large  $\gamma$ , however, both difference measures tend to be small.

Below we report on test runs of Algorithm IP when applied to  $P1$  and  $P2$ . The parameters had values  $q = 1.5$ ,  $\tau_1 = 10$ ,  $\tau_3 = 0.999$ ,  $\tau = 1e6$ . The stopping rule for the outer iteration is as before.

$P1$ . The infeasible version of Algorithm IP requires 12 outer iterations and one inner iteration per outer iteration. In particular the criterion  $(y_{k+1}, \lambda_{k+1}) \in \mathcal{N}(\gamma_k)$  was always satisfied within one inner iteration. The feasible version of Algorithm IP stops after 11 iterations. With respect to inner iterations in the feasible case we note that more than one or two inner iterations were necessary only in the last three outer iterations with 3, 4, and 6 inner iterations, respectively. For both runs, the behavior of the measures  $\rho^F$  and  $\rho^C$  is shown in Figure 9. Note that the vertical scale is a logarithmic one. The left plot corresponds to the infeasible case. The feasibility measure  $\rho^F$  and the complementarity measure  $\rho^C$  are both convergent at a superlinear rate. In the feasible case, which is depicted in the right plot, we observe that  $\rho^C$  is only linearly convergent. In some iterations we have  $\rho_k^F > 0$ . However, the constraint violation is of the order of the machine precision and, thus, negligible.

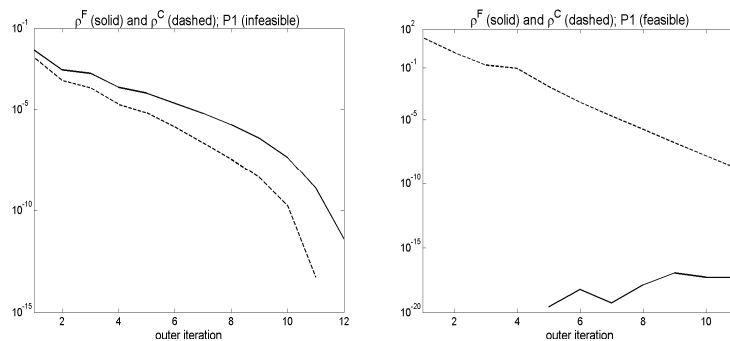


FIGURE 9. Behavior of the measure  $\rho^F$  (solid) and  $\rho^C$  (dashed) for  $P1$ ; left plot – infeasible case; right plot – feasible case.

$P2$ . For this test problem the infeasible version of Algorithm IP required 17 iterations with one inner iteration per outer iteration. The feasible version needed 6 outer iterations and 9 inner iterations.

Compared to the exact path-following strategy of Algorithm EP, the inexact path-following concept of Algorithm IP is in many cases more efficient. In Table 3 we provide the number of outer and inner



iterations for exact vs. inexact path following. In parenthesis we write the number of inner iterations.

	Infeasible case		Feasible case	
	$P1$	$P2$	$P1$	$P2$
EP	4 (15)	4 (11)	5 (44)	4 (10)
IP	12(12)	17 (17)	11(24)	6 (9)

TABLE 3. Comparison of iteration counts between exact and inexact path following.

## REFERENCES

- [1] M. Bergounioux, M. Haddou, M. Hintermüller, and K. Kunisch. A comparison of a Moreau-Yosida-based active set strategy and interior point methods for constrained optimal control problems. *SIAM J. Optim.*, 11(2):495–521 (electronic), 2000.
- [2] X. Chen and P. Tseng. Non-interior continuation methods for solving semi-definite complementarity problems. *Math. Program.*, 95(3, Ser. A):431–474, 2003.
- [3] A. V. Fiacco and G. P. McCormick. *Nonlinear Programming*, volume 4 of *Classics in Applied Mathematics*. Society for Industrial and Applied Mathematics (SIAM), Philadelphia, PA, second edition, 1990. Sequential unconstrained minimization techniques.
- [4] A. Forsgren, P. E. Gill, and M. H. Wright. Interior methods for nonlinear optimization. *SIAM Rev.*, 44(4):525–597 (electronic) (2003), 2002.
- [5] W. Hackbusch. *Theorie und Numerik elliptischer Differentialgleichungen*. Teubner Verlag, Stuttgart, 1986.
- [6] M. Hintermüller. Inverse coefficient problems for variational inequalities: optimality conditions and numerical realization. *M2AN Math. Model. Numer. Anal.*, 35(1):129–152, 2001.
- [7] M. Hintermüller, K. Ito, and K. Kunisch. The primal-dual active set strategy as a semi-smooth Newton method. *SIAM J. Optim.*, 13(3):865–888, 2003.
- [8] K. Ito and K. Kunisch. Optimal control of elliptic variational inequalities. *Appl. Math. Optim.*, 41(3):343–364, 2000.
- [9] K. Ito and K. Kunisch. Semi-smooth Newton methods for state-constrained optimal control problems. *Systems Control Lett.*, 50(3):221–228, 2003.
- [10] K. Ito and K. Kunisch. Semi-smooth Newton methods for variational inequalities of the first kind. *M2AN Math. Model. Numer. Anal.*, 37(1):41–62, 2003.
- [11] M. Ulbrich. Semismooth Newton methods for operator equations in function spaces. *SIAM J. Optim.*, 13(3):805–842 (electronic) (2003), 2002.
- [12] R. J. Vanderbei. *Linear Programming*. International Series in Operations Research & Management Science, 37. Kluwer Academic Publishers, Boston, MA, second edition, 2001. Foundations and extensions.
- [13] M. Weiser. Interior point methods in function space. ZIB-Report 03-35, Konrad-Zuse Zentrum für Informationstechnik Berlin, 2003.

- [14] S. J. Wright. *Primal-dual Interior-Point Methods*. Society for Industrial and Applied Mathematics (SIAM), Philadelphia, PA, 1997.
- [15] Y. Ye. *Interior Point Algorithms*. John Wiley & Sons Inc., New York, 1997. Theory and analysis, A Wiley-Interscience Publication.